Green Chemistry

ROYAL SOCIETY OF CHEMISTRY

CRITICAL REVIEW

View Article Online
View Journal | View Issue

Cite this: *Green Chem.*, 2025, **27**, 11561

Electrolyte engineering for low-temperature aqueous batteries: strategies, mechanisms, and perspectives

Jian Wang,†[a] Linlong Zuo,†[a] Ya He,[a] Ziming Wan,[a] Pengfei Yao,[a] Junrun Feng, *[a] Lin Sheng*[b] and Zhangxiang Hao *[a]

Aqueous batteries offer inherent safety and environmental advantages, yet their deployment is critically constrained by severe performance degradation below 0 °C, where capacity losses exceed 50–80% and complete failure occurs below −20 °C. This limitation significantly restricts applications in rapidly expanding cold-climate sectors including Arctic operations and winter electric mobility. This comprehensive review presents a systematic analysis of electrolyte modification strategies through four primary approaches: concentration engineering, inorganic additives, organic additives, and gel electrolyte architectures. Unlike previous reviews focusing on individual techniques, this work establishes a holistic framework integrating molecular-level mechanisms with macroscopic performance outcomes. Recent advances demonstrate remarkable progress: concentration engineering enables operation to −70 °C through higher concentration mechanisms, inorganic additives achieve stable cycling at −60 °C *via* hydrogen bonding disruption, organic additives provide multi-functional enhancement to −55 °C through coordinated solvation engineering, and gel electrolytes deliver robust performance at −50 °C through synergistic polymer-additive interactions. Advanced characterization reveals optimal performance requires multi-scale synergistic regulation across molecular solvation environments, interfacial processes, and bulk transport properties. Critical gaps include incomplete understanding of interfacial evolution during thermal cycling and limited predictive capability for multi-component optimization. This analysis establishes fundamental design principles and identifies priority research directions for translating laboratory breakthroughs into commercially viable low-temperature aqueous battery technologies.

Received 12th June 2025,
Accepted 29th August 2025

DOI: 10.1039/d5gc02967h

rsc.li/greenchem

Green foundation

(1) This review presents breakthrough green electrolyte strategies enabling aqueous batteries to operate at unprecedented low temperatures (−160 °C to −50 °C), replacing toxic organic electrolytes. Key innovations include sustainable "water-in-salt" mechanisms suppressing ice formation, bio-derived antifreeze molecules disrupting hydrogen bonding, and environmentally benign multi-component systems maintaining green chemistry principles.

(2) Unlike previous fragmented studies, this work establishes the first unified theoretical framework for low-temperature green battery design, revealing multi-scale synergistic regulation principles. Systematic structure–property correlations enable predictive electrolyte optimization, transforming sustainable energy storage from trial-and-error to knowledge-driven approaches for Arctic operations.

(3) This framework will enable rational design of next-generation cryogenic green electrolytes through predictive modeling. The identified mechanisms and bio-inspired design principles will guide development of sustainable additives for extreme environments, accelerating commercialization of safe battery technologies for polar regions.

1 Introduction

Aqueous batteries (ABs), encompassing lithium-ion, sodium-ion, potassium-ion, zinc-ion, and other metal-ion systems, have emerged as promising alternatives due to their inherent safety advantages, environmental compatibility, abundant raw material availability, and superior ionic conductivity in aqueous media.[1–6] However, the practical implementation of these systems faces a critical bottleneck in low-temperature

[a]*School of Science, School of Chip Industry, Hubei University of Technology, Wuhan, Hubei 430068, China. E-mail: fengjunrun@hbut.edu.cn, haozx@hbut.edu.cn*
[b]*School of Mechanical and Electronic Engineering, Suzhou University, Suzhou, Anhui 234000, China. E-mail: shenglin@ahszu.edu.cn*
†These authors contributed equally to this work.

environments, where performance degradation becomes severe below 0 °C, significantly limiting their deployment in high-latitude regions, polar research stations, cold-climate energy storage facilities, and winter electric vehicle applications.[7–9] The growing demand for reliable energy storage in extreme environments, driven by expanding Arctic operations, increasing cold-region renewable energy projects, and the need for year-round electric mobility, has made the development of low-temperature aqueous batteries a strategic priority for achieving global energy security and climate goals.[8,10,11]

The performance degradation of aqueous batteries under low-temperature conditions represents a fundamental scientific and technological challenge that severely constrains their practical viability. Experimental studies have demonstrated that conventional aqueous battery systems experience dramatic capacity losses, often exceeding 50–80%, when operating temperatures drop below 0 °C, with complete failure frequently occurring at temperatures below −20 °C.[7,12,13] This performance deterioration manifests across multiple critical dimensions: ionic conductivity decreases by several orders of magnitude due to increased electrolyte viscosity and restricted ion mobility, charge transfer kinetics become severely limited by enhanced activation barriers, and ice crystal formation can cause irreversible structural damage to battery components.[12,14,15]

The underlying mechanisms stem from water's unique molecular properties, particularly the strengthening of hydrogen bonding networks at reduced temperatures, which fundamentally alters electrolyte structure and ion transport pathways.[16–20] Current commercial aqueous battery technologies remain largely ineffective for applications requiring operation below −10 °C, creating a significant technological gap in cold climates where energy storage demand is rapidly growing.[21–23] This limitation has become increasingly urgent as climate change drives energy infrastructure development in polar regions and the electrification of cold-climate transportation systems demands reliable low-temperature energy storage solution.[24]

The rapidly growing research interest in low-temperature aqueous batteries is evidenced by the exponential increase in scientific publications, with cryogenic battery studies rising from 215 papers in 2021 to 383 papers in 2024, while aqueous cryogenic battery research specifically grew from 155 to 283 publications over the same period (Fig. 1A and B). This surge in research activity reflects the scientific community's increasing focus on electrolyte engineering as the most promising and versatile approach for enhancing aqueous battery performance under extreme conditions. Current research strategies have evolved along four primary pathways: concentration regulation through "water-in-salt" formulations that fundamentally alter ion–water interactions and suppress ice formation, inorganic additive incorporation utilizing high-charge-density cations and structure-breaking anions to disrupt hydrogen bonding networks, organic additive integration leveraging functional molecules to modify solvation structures and interfacial properties, and gel electrolyte construction that combines polymer networks with strategic additives to achieve synergistic performance enhancement.

Statistical analysis of recent literature reveals that organic additives dominate current research efforts (62%), followed by concentration regulation (28%), inorganic additives (6%), and gel electrolytes (4%) (Fig. 1C), reflecting both the versatility of organic molecules and the accessibility of this modification approach.[7,25–28] Recent breakthroughs have demonstrated remarkable progress across different battery chemistries and temperature ranges, with milestone achievements including zinc-based systems operating at −70 °C (7.5 M $ZnCl_2$, 2000 cycles), −50 °C ($ZnCl_2$-αDG, 10 000 cycles), alongside sodium-based systems achieving stable cycling at −60 °C with thousands of cycles (Fig. 1D).[4,28–32] However, significant challenges persist in translating these laboratory achievements to practical applications. Key obstacles include the cost-effectiveness of ultra-high concentration electrolytes, scalability of complex multi-component systems, and trade-offs between low-temperature performance and other critical metrics such as energy density and safety.[2,33] Furthermore, the mechanistic understanding of how different modification strategies interact at

Jian Wang

Jian Wang received his Bachelor of Science from Hubei Polytechnic University in June 2021. After that, he studied under the guidance of Professor Hao Zhangxiang of Hubei University of Technology and joined the Green Battery Innovation Laboratory to study for a master's degree. His research focuses on electrolyte additives in secondary rechargeable battery systems.

Linlong Zuo

Linlong Zuo received his Bachelor of Engineering from Chuzhou University in June 2022. Then he learnt from Prof. Zhangxiang Hao's group in Hubei University of Technology and joined the Green Battery Innovation Laboratory to study for a master's degree. His research focuses on electrolyte additives in secondary rechargeable battery systems at low temperatures.

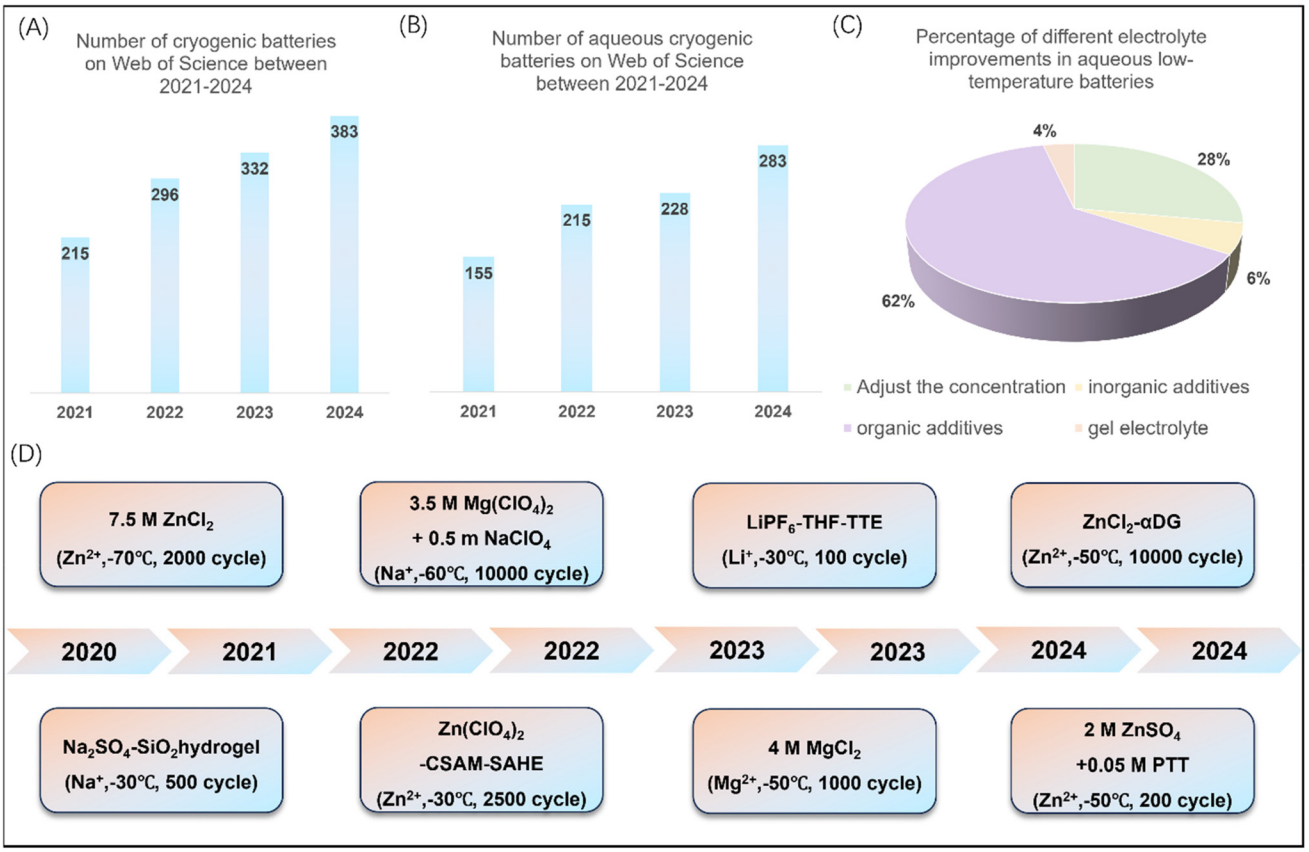

Fig. 1 (A) Number of low temperature batteries on web of science 2021–2024. (B) Number of low temperature aqueous batteries on web of science 2021–2024. (C) Percentage of different additive categories in low-temperature aqueous batteries. (D) Development of low-temperature water-based batteries in 2020–2024.

the molecular level remains incomplete, limiting rational design of optimized electrolyte systems.[34–36] The field has reached a critical juncture where systematic analysis and integration of existing approaches are essential for advancing toward commercially viable low-temperature aqueous battery technologies.[15,37,38]

This comprehensive review provides a systematic and critical analysis of electrolyte modification strategies for low-temperature aqueous batteries, offering both fundamental insights and practical guidance for this rapidly evolving field. Unlike previous reviews that focus on individual modification approaches, this work presents a holistic framework integrat-

Pengfei Yao

Dr Pengfei Yao received his PhD from University of Science and Technology of China in November 2023. He has recently joined the Green Battery Innovation Laboratory and has become a Lecturer at Hubei University of Technology (HBUT). His research interests mainly focus on the conversion and utilization of hydrogen, including the design of electrode catalysts and the related reaction mechanism investigation for electrolysis of water and proton exchange membrane fuel cell.

Junrun Feng

Prof Junrun Feng received his PhD from University College London (UCL) in May 2023. He currently joined the Green Battery Innovation Laboratory and became an associate professor in Hubei University of Technology (HBUT). His research interest mainly focuses on characterization of electrode and electrode/electrolyte interface in secondary rechargeable battery systems.

ing molecular-level mechanisms with macroscopic performance outcomes, enabling deeper understanding of structure–property relationships in low-temperature electrolyte systems.[39–41] We begin by elucidating the fundamental mechanisms underlying low-temperature performance degradation from thermodynamic and molecular perspectives, providing the theoretical foundation for subsequent discussions (Section 2). The core systematically examines four major electrolyte modification strategies—concentration regulation, inorganic additives, organic additives, and gel electrolytes—with emphasis on their molecular mechanisms, synergistic effects, and practical implementation considerations (Section 3). Through comprehensive analysis of key performance parameters across different battery chemistries and temperature ranges, we identify critical design principles and performance benchmarks to guide future research directions.[42,43] By synthesizing current knowledge and identifying research gaps, this work aims to accelerate development of practical low-temperature aqueous battery technologies and provide a roadmap for reliable energy storage in extreme environments.[44,45] The insights presented are expected to benefit researchers, engineers, and policy-makers working toward sustainable energy solutions in cold climates.[12,14]

2 Problems and mechanisms of low-temperature aqueous batteries

Aqueous batteries have attracted considerable attention for large-scale energy storage applications due to their inherent safety and environmental compatibility. However, significant performance deterioration at low temperatures (typically below 0 °C) severely limits their application in high-latitude regions and cold-climate environments.[46] This poor low-temperature performance primarily originates from the unique physicochemical properties of water-based electrolytes, which undergo fundamental structural and dynamic changes under sub-zero conditions. Understanding these fundamental limitations requires systematic analysis from both thermodynamic and molecular perspectives to develop effective mitigation strategies.[47]

The reaction kinetics in aqueous batteries can be fundamentally understood through the temperature-dependent Arrhenius relationship:

$$k = A \exp\left(-\frac{E_a}{RT}\right)$$

where k represents the reaction rate constant, A is the pre-exponential factor reflecting collision frequency, E_a represents the activation energy barrier, R is the universal gas constant, and T is the absolute temperature.[29,48,49] This relationship quantitatively describes how reaction rates exponentially decrease with declining temperature, as the fraction of molecules with sufficient energy to overcome the activation barrier diminishes.[42,50] In aqueous systems, the temperature dependence is further complicated by water's unique properties: the dielectric constant increases significantly at lower temperatures, enhancing ion–dipole interactions and affecting ion dissociation, while water's viscosity exhibits exponential increases that substantially impede ion mobility.[26,51–53]

The synergistic effect of these temperature-dependent properties manifests in dramatic changes in activation energy for ion transport processes. In conventional aqueous electrolytes, activation energies typically rise from 40–50 kJ mol^{-1} at ambient temperature to over 70–80 kJ mol^{-1} below 0 °C.[54] However, strategic electrolyte modifications can significantly reduce these energy barriers. For example, $ZnCl_2$-based systems exhibit concentration-dependent behavior, with activation energies starting at 51.7 kJ mol^{-1} at room temperature in dilute solutions. At high concentrations, however, the activation energy does not increase significantly even at low temperatures. Multi-salt strategies prove even more effective: Ca^{2+}-modified $ZnCl_2$ electrolytes achieve activation energies as low as 20.3 kJ mol^{-1} at −50 °C, while $ZnCl_2$–LiCl mixtures demonstrate similar improvements.[20] These enhanced energy barriers directly impact both bulk ion transport and interfacial charge transfer processes, but demonstrate that rational electrolyte

Lin Sheng

Dr Lin Sheng received her PhD degree from the University College London (UCL) in 2022. From 2022, she works in the School of Mechanical and Electronic Engineering, Suzhou University. Her current research focuses on Mg–S battery, solid-state battery and electrodes for Zinc-ion battery.

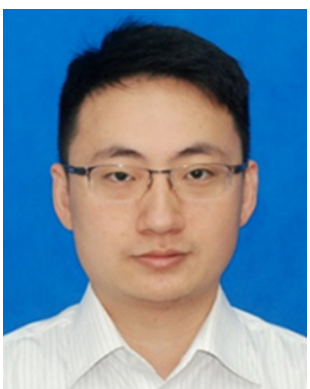

Zhangxiang Hao

Prof. Dr Zhangxiang Hao received his PhD degree from Huazhong University of Science and Technology (HUST). He then worked as a postdoctoral researcher in the University College London (UCL) for more than three years. He joined Hubei University of Technology (HBUT) in 2021 and led the Green Battery Innovation Laboratory group, which focuses on batteries of energy storage and conversion.

design can mitigate kinetic limitations at low temperatures.[3,55–57]

At the molecular level, the unique behavior of aqueous electrolytes originates from water's distinctive molecular architecture.[14,58,59] The water molecule exhibits a bent structure with an H–O–H angle of 104.5°, where the electronegative oxygen atom bears a partial negative charge while the hydrogen atoms carry partial positive charges.[16,20,60–63] This asymmetric charge distribution enables the formation of hydrogen bonds, where each water molecule can potentially form four hydrogen bonds (two as a donor and two as an acceptor). Under ambient conditions, water molecules participate in an extensive hydrogen bonding network characterized by dynamic equilibrium.[20,64,65] Each water molecule forms an average of 3.3 hydrogen bonds with neighboring molecules, with bond lifetimes in the picosecond range.[1] This dynamic network structure, where approximately 99% of water molecules are integrated into the hydrogen bonding framework, facilitates rapid molecular reorientation and ion transport.[18,19,29]

As temperature decreases, the thermal energy available for molecular motion diminishes, fundamentally altering the hydrogen bonding dynamics.[1,17] The reduced molecular mobility leads to increased hydrogen bond lifetime and strength, promoting the formation of more stable tetrahedral coordination structures.[34] This structural evolution follows a hierarchical process. Initially, local water clusters with enhanced hydrogen bonding emerge.[66] These clusters subsequently grow and interconnect, forming extended networks that serve as precursors for ice nucleation.[19,67] The progression toward more ordered structures significantly impacts electrolyte properties through multiple mechanisms, such as restricting ion transport channels, increasing the energy barrier for hydrogen bond reorganization during ion migration, and enhancing the stability of ion hydration shells that must be partially disrupted during electrode reactions.[68–70]

The ion-specific effects in aqueous electrolytes can be systematically understood through the Hofmeister series (CO_3^{2-} > SO_4^{2-} > F^- > Cl^- > Br^- > NO_3^- > I^- > ClO_4^- > SCN^-), which fundamentally reflects the competition between ion–water interactions and water–water hydrogen bonding.[71,72] This series correlates strongly with ion properties such as charge density, polarizability, and ionic radius, determining their ability to influence water's hydrogen bonding network. The hydration behavior of ions follows distinct patterns based on their charge density and size.[42,73,74] Small ions with high charge density (such as CO_3^{2-} and SO_4^{2-}) generate intense electric fields at the ion surface, leading to strongly bound primary hydration shells with relatively long water residence times.[75,76] These ions promote favorable water stability and structural organization, classifying them as "structure makers".[77] Conversely, large monovalent ions with low charge density exhibit weaker electric fields, resulting in more loosely bound hydration structures with shorter water residence times. These ions disrupt the native hydrogen bonding network and are classified as "structure breakers".[39,41,78]

For multivalent ions prevalent in aqueous batteries, particularly Zn^{2+} and Al^{3+}, the hydration structure exhibits complex multilayer characteristics.[2,46,79,80] These ions typically form well-defined primary hydration shells with coordination numbers of 6 (Zn^{2+}) and 6–8 (Al^{3+}).[4,5,29,53,71] At low temperatures, the enhanced stability of these hydration structures significantly impacts electrode reactions, as the energy required for partial dehydration during charge transfer increases substantially. This temperature-dependent strengthening of ion hydration becomes a critical factor limiting battery performance, particularly affecting the kinetics of electrode reactions where partial dehydration is necessary for electron transfer processes.

The combined effects of these temperature-dependent phenomena create multiple challenges for aqueous battery operation at low temperatures. From a kinetic perspective, the exponential decrease in reaction rates following the Arrhenius relationship fundamentally limits all electrochemical processes.[29,48,49] This limitation is exacerbated by the increased water viscosity and enhanced hydrogen bonding network, which significantly restrict ion mobility in the bulk electrolyte. The strengthened water structure and more stable ion hydration shells, particularly for multivalent ions, create additional energy barriers for both ion transport and interfacial charge transfer.[7] These molecular-level mechanisms manifest in several key performance metrics: higher internal resistance due to restricted ion transport, increased charge transfer resistance from enhanced hydration effects, and reduced capacity utilization from kinetic limitations. Moreover, the tendency toward ice formation near 0 °C introduces additional risks of electrolyte freezing and mechanical damage to battery components. Understanding these fundamental limitations provides crucial insights for developing effective strategies to enhance low-temperature performance, such as electrolyte engineering to modify water structure, interface design to facilitate charge transfer, and architectural innovations to maintain ion transport pathways (Fig. 2).[28] These approaches will be discussed in detail in the following sections.

3 Electrolyte modification classification

Building upon the understanding of low-temperature limitations in aqueous systems, electrolyte engineering has emerged as a primary strategy to enhance battery performance under extreme conditions. The fundamental challenge lies in water's extensive hydrogen bonding network, which leads to high freezing points and severely restricted ion transport at low temperatures.[7] To address these limitations, recent research has focused on strategic modifications of electrolyte composition and structure to disrupt water's hydrogen bonding network and suppress ice nucleation.[36] Based on existing studies, the approaches can be systematically categorized into four major strategies: regulation of electrolyte con-

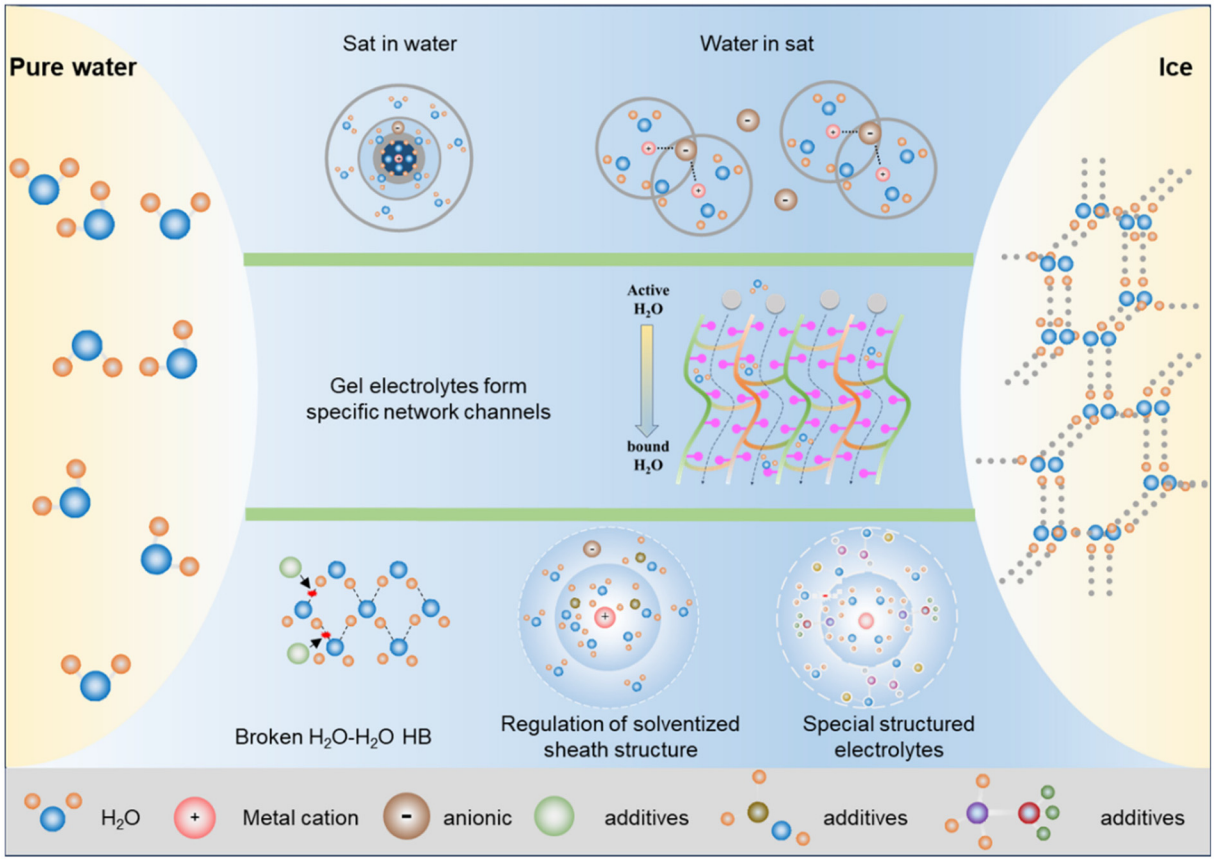

Fig. 2 Schematic diagram for adjusting electrolyte to lower freezing point.

centration, inorganic additives, organic additives, and gel electrolytes, each targeting specific aspects of the low-temperature challenges (Fig. 3).[25,81,82]

3.1 Concentration engineering strategies

In aqueous battery systems, the interaction between metal cations and water molecules is dominated by strong electrostatic forces, leading to the formation of well-defined solvation structures.[3,46,55,56,83,84] Typically, the first coordination shell consists of six water molecules arranged in an octahedral geometry around the metal cation.[85] This primary solvation significantly alters the hydrogen bonding network and dielectric environment of the electrolyte, as the water molecules within the coordination sphere are strongly bound by the cation's charge field and unable to participate in the normal water hydrogen bonding network.

The relative abundance of various ion-pair species varies significantly with concentration, each exhibiting unique effects on the electrolyte's physicochemical characteristics.[86] The progression of ion–ion interactions across different concentration regimes exhibits three characteristic configurations: In dilute solutions (<2 M), solvent-separated ion pairs (SSIPs) predominate, where fully hydrated metal cations (*e.g.*, $[M(H_2O)_6]^{2+}$) remain isolated from anions by intact solvent shells, leaving a substantial population of free water molecules in the bulk solution.[87,88] As concentration increases, contact ion pairs (CIPs) emerge through partial displacement (1–-2 molecules) of coordinated water by anions.[40,89] At higher concentrations, extensive dehydration (≥3 water molecules) leads to polynuclear aggregates and complex ionic associations.[33,41,90] In dilute systems, the freezing point depression is limited and follows the classical relationship:

$$\Delta T_f = T_{water} - T_{soln} = K_f \cdot m$$

where ΔT_f = freezing point depression, T_{water} = thermodynamic freezing point of water = 0 °C, T_{soln} = freezing point of the solution, K_f = freezing point depression constant (= 1.86 °C kg mol^{-1}, water), and m = molar concentration of the solution.[40,53] For example, a 1 M LiCl solution has a freezing point of −3.72 °C due to the presence of two molar ions (Li^+ and Cl^-). However, as salt concentration increases beyond dilute regimes, the system behavior deviates significantly from this simple relationship.[40,41] Anions progressively incorporate into the metal ion solvation shells, forming complex metal ion-$(anion)_m(H_2O)_n$ clusters that effectively immobilize additional water molecules. This structural transformation achieves two critical effects: substantial depletion of free water molecules and intensification of ion–water interactions, both of which dramatically disrupt the native hydrogen bonding network.[39,40] In highly concentrated "water-in-salt" systems,

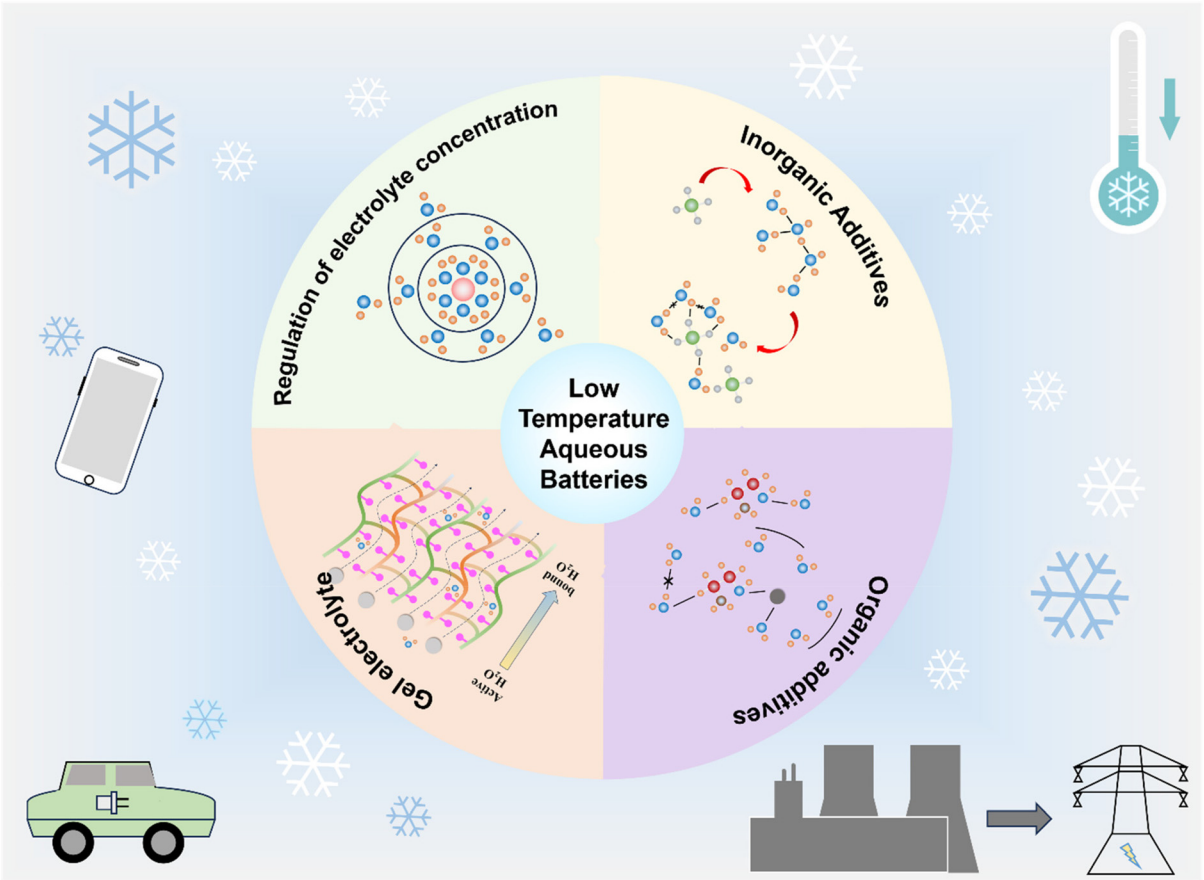

Fig. 3 Strategy for low-temperature aqueous batteries – synergistic effects of concentration engineering, additive interfaces, and gel electrolyte frameworks.

where the salt content exceeds that of water by both mass and volume, nearly all water molecules become coordinated with ions, leaving minimal free water in solution.[69,91,92] Remarkably, this mechanism can induce freezing point depressions exceeding several tens of degrees Celsius – a profound modification of water's fundamental physical properties.

The practical implementation of this principle has been successfully demonstrated in aqueous potassium-ion batteries. Li *et al.* utilized a 22 M KCF_3SO_3 electrolyte, where Raman spectroscopy revealed a distinct peak at 3531 cm^{-1}, confirming the strong solvation of K^+ ions at such high concentrations (Fig. 4A). This concentrated electrolyte not only expanded the electrochemical stability window to approximately 3.0 V but also effectively suppressed electrode dissolution (Fig. 4B). The system achieved an impressive energy density of 80 Wh kg^{-1} when paired with a manganese-rich Prussian blue cathode and an organic PTCDI anode, while maintaining stable operation at −20 °C (Fig. 4C and D).[2] Comparable performance enhancements have been reported across various concentrated single-salt systems, as well as in other aqueous battery chemistries such as sodium-ion, lithium-ion, and zinc-ion batteries.[93,94] These findings highlight the universal benefits of high-concentration electrolytes in improving both electrochemical performance and low-temperature stability.

The relationship between electrolyte concentration and low-temperature performance exhibits complex nonlinear characteristics that challenge simple theoretical predictions. While ultrahigh concentrations can induce remarkably low freezing points in certain electrolytes, this effect is not universally observed across all systems. The intricate interplay between ionic interactions and solution properties creates competing effects: elevated concentrations with strong ion pairing may substantially increase electrolyte viscosity, while reduced solubility at low temperatures can trigger salt precipitation.[36,69,91] These competing factors create an optimization challenge where concentration alone cannot reliably predict performance outcomes.

The $ZnCl_2$ electrolyte system exemplifies this complexity while demonstrating exceptional potential for low-temperature applications. The Zn^{2+} cation, characterized by its high charge density and small ionic radius, profoundly restructures the aqueous environment through intense electrostatic interactions.[95,96] This drives a concentration-dependent speciation of zinc complexes, evolving from simple hydrated ions $[Zn(H_2O)_6]^{2+}$ in dilute solutions to diverse coordination struc-

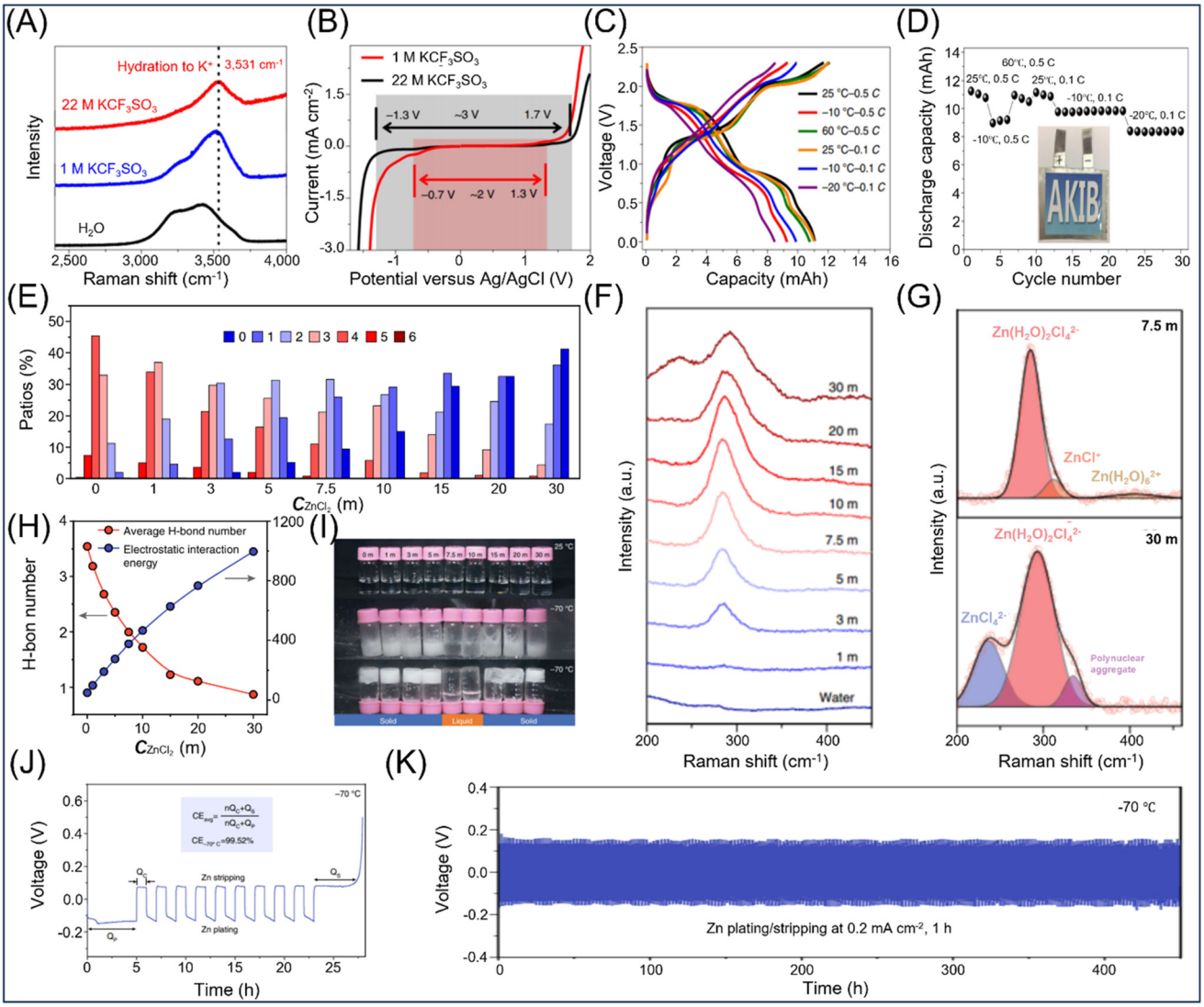

Fig. 4 (A) Raman spectra of different concentrations of KCF_3SO_3 electrolyte. (B) Electrochemical window for 1 M and 22 M KCF_3SO_3 electrolytes. (C) Typical charge/discharge curves of KFeMnHCF-3565//22 M KCF_3SO_3//PTCDI pouch batteries at different rates and temperatures. (D) KFeMnHCF-3565//22 M KCF_3SO_3//PTCDI pouch batteries at different rates and temperatures and cycling performance. Reproduced from ref. 2 with permission from Nature Publishing Group, copyright 2019. (E) The proportion of different H-bound water molecules at different electrolyte concentrations. (F) Raman spectra of $ZnCl_2$ electrolyte with different concentrations. (G) Peak fitting of Raman spectra of 7.5 and 30 M $ZnCl_2$ electrolytes. (H) Hydrogen bond number and electrostatic interaction energy at different concentrations. (I) Optical photographs of different concentrations of $ZnCl_2$ at different temperatures. (J) Voltage distribution of zinc plating/stripping in Zn||Cu cells at low temperatures. (K) Cycling performance of Zn||Zn cells at low temperatures. Reproduced from ref. 29 with permission from Nature Publishing Group, copyright 2020.

tures such as $ZnCl^+$, $Zn(H_2O)_2Cl_4^{2-}$, and multicore aggregates at higher concentrations.[96]

The progressive disruption of water's hydrogen bonding network with increasing concentration is clearly demonstrated through structural analysis. As illustrated in Fig. 4E, pure water is dominated by tetrahedrally coordinated water molecules with four hydrogen bonds, whereas in 7.5 M $ZnCl_2$, water molecules primarily form two hydrogen bonds. At 30 M, most water molecules lose their hydrogen bonds entirely, confirming the progressive breakdown of the network. Raman spectroscopy results (Fig. 4F and G) further reveal that at 7.5 M concentration, $ZnCl_4^{2-}$ complexes with multicore aggregates become predominant, facilitating efficient ionic conduction while maintaining structural stability at low temperatures.[29]

Critically, the system exhibits optimal performance at intermediate concentrations rather than maximum concentrations. As illustrated in Fig. 4H and I, the interplay between modified hydrogen bonding networks and ionic structural changes results in the lowest freezing point at intermediate concentrations, with only these solutions remaining liquid at −70 °C. This non-monotonic behavior reflects the balance between beneficial hydrogen bond disruption and detrimental viscosity increases. Electrochemical validation by Zhang *et al.* confirms these findings, with 7.5 M $ZnCl_2$ maintaining exceptional per-

formance (coulombic efficiency >97%) even at −70 °C in Zn–Cu cells, while Zn-PANI cells demonstrated stable operation down to −70 °C (Fig. 4J and K).[29] These observations align with behavior patterns observed in other multivalent systems (Mg^{2+}, Al^{2+}), establishing intermediate concentrations as providing the optimal balance between structural modification and electrochemical performance for low-temperature applications.[31,97]

Beyond single-salt strategies, multi-salt electrolyte systems have emerged as an effective approach to circumvent individual salt limitations while achieving synergistic performance enhancements. This strategy addresses the inherent constraints of single-salt systems, such as solubility limits and suboptimal ion coordination, by combining complementary salts that collectively optimize electrolyte properties.

The approach has demonstrated success in lithium-based electrolytes, where the judicious combination of LiTFSI (21 M) and LiOTf (7 M) yields an ultrahigh total salt concentration of 28 m while preserving the beneficial characteristics of both salts.[33] The resulting binary system maintains excellent phase stability with a liquidus temperature of −21.4 °C, comparable to single-salt systems, while sustaining ionic conductivity in the favorable 6–8 mS cm^{-1} range.[33] This demonstrates that multi-salt formulations can achieve concentration levels that would be impossible with individual components due to solubility constraints. These multi-component systems leverage the distinct advantages of different anions, such as varying structure-making/breaking properties and coordination preferences, to create electrolytes with superior overall properties compared to their single-salt counterparts.

Although significant adjustments to electrolyte concentration can enable low-temperature battery applications, the sharp cost increases from higher concentrations remain a major constraint on large-scale commercialization potential.

Quantitative cost analysis reveals significant differences among electrolyte systems (Fig. S1). For zinc salts per 100 g: $Zn(OAc)_2$ (£25.5) offers the most economical option, followed by $ZnCl_2$ (£57.41), $ZnSO_4$ (£57.35), $Zn(ClO_4)_2$ (£68.4), $Zn(BF_4)_2$ (£243.1), and $Zn(CF_3SO_3)_2$ (£378.55). However, achieving low-temperature performance through ultra-high concentrations (30 M *vs.* 1 M) results in impressive cost increases (over dozens of times) due to dramatically higher material requirements.

The economic challenge extends beyond raw material costs. High-concentration electrolyte preparation requires specialized processing to maintain solute dissolution and prevent crystallization through controlled environmental conditions, introducing additional operational costs that further impact commercialization viability.[33,38,98]

Concentration engineering in low-temperature aqueous batteries enhances low-temperature performance by adjusting the salt concentration in the electrolyte, with the core mechanism lying in altering ion–water interactions and hydrogen bond networks. In dilute solutions, the classical freezing point depression law applies; as concentration increases, the morphology of ion pairs gradually transitions from solvent-separated to contact-type and multi-nuclear aggregates, significantly reducing free water through the "salt-wrapped water" mechanism and effectively inhibiting ice crystal formation.[20] Multi-salt systems overcome the solubility limitations of single salts through synergistic effects, maintaining low freezing points while preserving good ionic conductivity.[29] However, in commercial applications, the significant cost differences between different electrolyte materials and the sharp increase in costs caused by elevated electrolyte concentrations remain key factors constraining the development of electrolyte concentration engineering.

3.2 Inorganic additive approaches

Inorganic additives offer a promising approach to improve the low-temperature performance of aqueous batteries by employing three distinct mechanisms. The high-charge-density cations effectively disrupt the hydrogen-bonding network of water molecules, while the anions modify the chemical environment of water through their specific physicochemical properties. Furthermore, strategic combinations of different salts can create synergistic effects that enhance overall electrolyte performance.

Multivalent cations have emerged as particularly effective inorganic additives for modifying aqueous electrolyte structures, owing to their high ionic potential and strong polarization effects. These cations significantly reduce the population of active water molecules while depressing the electrolyte's freezing point.[99–101] Zhu *et al.* demonstrated this principle in a sodium-ion battery system by introducing magnesium perchlorate into sodium perchlorate solution. Building upon established concentration effects in electrolytes, their work revealed that the added salt not only effectively lowered the freezing point but also modulated hydrogen bonding networks. The key innovation lies in Mg^{2+} superior ionic potential compared to Na^+, enabling more efficient polarization of water molecules and competition with water clusters. This interaction increases molecular spacing and creates a distinctive local chemical environment, resulting in further freezing point depression (Fig. 5A).[4] Notably, the high-potential cation also enhanced ionic conductivity (Fig. 5B) while shifting the water population toward coordinated water at the expense of free water molecules (Fig. 5C). The synergistic combination of both ions proved particularly effective at suppressing strongly hydrogen-bonded water (SHW) formation – the precursor to ice crystallization – thereby achieving superior freezing point reduction (Fig. 5D and E).[4] These molecular-level modifications translated into remarkable electrochemical performance, enabling sodium-ion batteries to maintain stable cycling at extreme temperatures as low as −60 °C with excellent rate capability and cycle life (Fig. 5F).[4] Furthermore, Jiao *et al.* strategically introduced Ca^{2+} ions, which share similar physicochemical properties with Mg^{2+}, into the electrolyte system.[53] This innovative approach enabled the $Na_2CF_6(CN)_6$/C cell configuration to deliver an impressive specific capacity of 74.5 mAh g^{-1} at 1C rate while demonstrating exceptional cycling stability – maintaining performance over 6000 cycles even under harsh −30 °C operating conditions.[53]

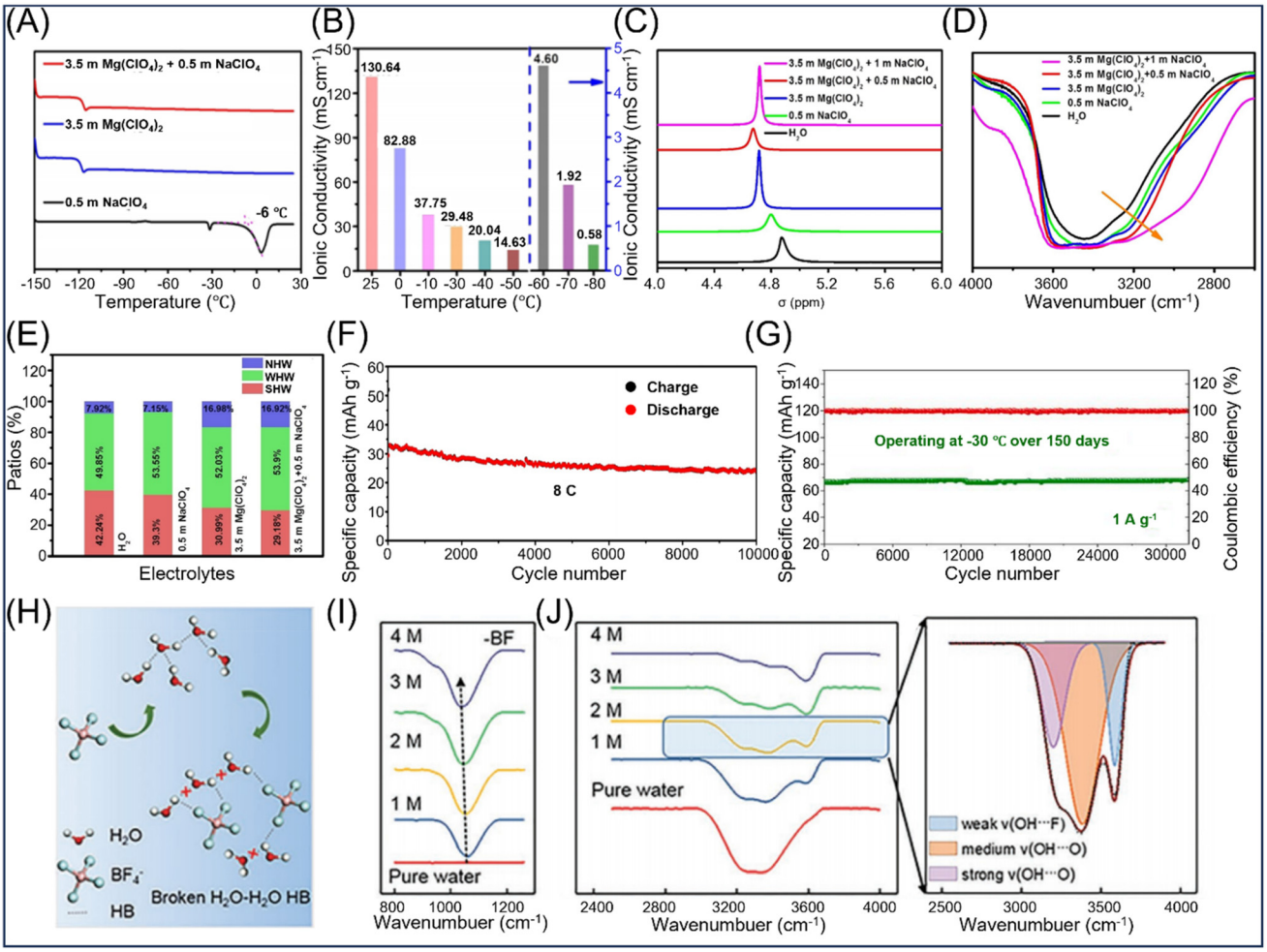

Fig. 5 (A) DSC results for 0.5 M $NaClO_4$, 3.5 M $Mg(ClO_4)_2$ and 3.5 M $Mg(ClO_4)_2$ + 0.5 M $NaClO_4$ electrolytes. (B) Comparison of ionic conductivity of 3.5 M $Mg(ClO_4)_2$ + 0.5 m $NaClO_4$ electrolyte at different temperatures. (C) ^1H NMR results of $Mg(ClO_4)_2$, $NaClO_4$ and mixed solutions of both. (D) FTIR results of $Mg(ClO_4)_2$, $NaClO_4$ and mixed solutions of both. (E) Proportion of water components in the electrolyte that have different hydrogen bonds. (F) Cycling performance of $NaTi_2(PO_4)_3$@C||AC full cell at 8C (1C = 133 mA g^{-1}) and −60 °C. Reproduced from ref. 4 with permission from Wiley-VCH, copyright 2022. (G) Cycling performance of AZHCs device at 1 A g^{-1} and −30 °C. Reproduced from ref. 25 with permission from Elsevier, copyright 2023. (H) Schematic representation of a BF_4^- anion disrupting the hydrogen bonding network of a pristine water molecule. FTIR results of (I) B–F bond and (J) O–H bond. Reproduced from ref. 71 with permission from Wiley-VCH, copyright 2021.

The effectiveness of anionic additives is equally noteworthy. Large-volume anions with low charge density exhibit superior solubility, while those with more constituent atoms and smaller electronegativity differences (resulting in longer bond lengths) can significantly expand the anion's effective volume. Such voluminous additives demonstrate enhanced freezing point depression capabilities.[39]

Pu *et al.* demonstrated this principle by introducing perchlorate anions into zinc sulfate electrolyte systems. While sulfate anions (SO_4^{2-}) maintain water's hydrogen bonding network as structural stabilizers – making the system more prone to freezing – the perchlorate anions act as structure breakers, disrupting hydrogen bonding order and further depressing the freezing point. Importantly, the high electrostatic potential of SO_4^{2-} is preserved, reducing Zn^{2+} solvation and optimizing electrolyte structure.[39] Through strategic incorporation of $Mg(ClO_4)_2$, this system synergistically combines cationic and anionic effects, achieving remarkable liquid mobility below −80 °C while maintaining 7.50 mS cm^{-1} ionic conductivity at −60 °C. The electrolyte demonstrates exceptional stability, delivering 32 000 cycles at −30 °C under 1 A g^{-1} with a specific capacity of 68 mAh· g^{-1} – far exceeding conventional $ZnSO_4$-based systems (Fig. 5G).[25] The potential of multicomponent strategies has been further validated in fluorine-based systems. Sun *et al.* revealed that BF_4^--based electrolytes (2 M HBF_4 + 2 M $Mn(BF_4)_2$) achieve unprecedented low-temperature stability through unique water structure modifications. Infrared spectroscopy analysis (Fig. 5I and J) demonstrated that BF_4^- anions establish a distinct hydrogen bonding network (Fig. 5H) enabling electrolyte fluidity below −160 °C while maintaining 0.21 mS cm^{-1} conductivity at −70 °C. This molecular-level optimization, combined with H^+ adsorption–

desorption at the ALO anode and MnO_2 reactions at the carbon felt cathode, yields exceptional device performance: 85 mAh g^{-1} capacity at −90 °C, and energy/power densities of 110 Wh kg^{-1} and 1650 W kg^{-1} at −60 °C.[71]

The evolution of inorganic additive strategies – from single-cation modifications (Mg^{2+}, Ca^{2+}) to sophisticated multi-component systems ($Mg(ClO_4)_2$-$ZnSO_4$, HBF_4-$Mn(BF_4)_2$) – demonstrates systematic progress in addressing low-temperature challenges in aqueous batteries.[4,25,71,102] These advances have expanded the practical temperature window from conventional low temperatures (−30 °C) to ultra-low conditions (−60 °C), while maintaining key performance metrics including ionic conductivity (0.21–7.50 mS cm^{-1}) and long-term stability (>30 000 cycles).[25,71] The success across different battery chemistries highlights the versatility of inorganic additives in modifying water structure and interfacial properties, providing valuable design principles for next-generation low-temperature energy storage systems. Future developments may focus on understanding the complex interplay between multiple ionic species and establishing predictive models for optimal additive combinations. In Table S1, we summarize the data regarding the use of inorganic additives at low temperatures to improve battery performance.

3.3 Organic additive systems

Organic additives represent a versatile class of strategies to enhance the low-temperature performance of aqueous batteries through multiple synergistic mechanisms.[100,103–105] These additives operate by regulating ion solvation environments through direct coordination, disrupting water's hydrogen bonding network, and promoting protective interfacial layer formation on electrode surfaces.[93,104] The effectiveness of organic additives stems from their diverse functional groups, which can be systematically categorized into three main classes: highly polar molecules (*e.g.*, formamide,[26,106,107] DMSO[7,10,81]) that provide strong hydrogen bonding interactions, hydroxyl-containing compounds (*e.g.*, alcohols,[32] glycols[52,67,108] saccharides[74]) that offer multiple coordination sites, and low-polarity solvents (*e.g.*, ethers[28,42]) that enable hierarchical solvation engineering. Unlike inorganic additives that primarily rely on ionic effects, organic molecules can simultaneously address multiple electrolyte challenges: forming stable coordination structures with cations to facilitate ion transport, reducing free water content to suppress parasitic reactions, modifying hydrogen bonding networks to depress freezing points, and contributing to stable solid electrolyte interphase (SEI) formation for enhanced electrode stability. This multifunctional capability has made organic additives particularly attractive for developing comprehensive solutions to low-temperature battery operation.[28,67,74,109,110] In Table S2, we summarize the data regarding the use of organic additives to improve battery performance at low temperatures.

Among various organic additives, formamide (FA) exemplifies the effectiveness of polar amide compounds for low-temperature aqueous battery applications. The unique molecular architecture of FA features dual functional groups: a carbonyl group (C═O) acting as a hydrogen bond acceptor and an amine group (–NH_2) serving as a hydrogen bond donor.[26,106,107] This dual functionality enables FA to establish "two-site anchored" hydrogen bonding interactions (C═O···H–O and N–H···O) with water molecules, effectively disrupting water's rigid tetrahedral network and replacing it with a more thermodynamically stable structure. Infrared and Raman spectroscopy (Fig. 6A–D) confirm this structural transformation, revealing how FA fundamentally alters water organization at the molecular level (Fig. 6E).[26] The practical benefits of this molecular engineering have been demonstrated across multiple battery systems. You *et al.* developed a 0.4 M $Zn(OAc)_2$/FA–H_2O electrolyte that suppresses water crystallization below −40 °C while forming novel solvation complexes $[Zn(H_2O)_m(FA)_n(OAc)_k]^{(2-k)+}$. This system delivered exceptional performance in Zn||PANI cells: 107 mAh g^{-1} capacity with remarkable stability over 22 000 cycles at −30 °C, and maintained 80 mAh g^{-1} through 6000 cycles even under extreme conditions (−40 °C, 5 A g^{-1}).[26] Similar enhancements have been reported in zinc sulfate systems and concentrated sodium electrolytes, where FA addition enabled stable operation at −50 °C, demonstrating the broad applicability of amide-based modification strategies.[106,107]

Beyond amide-based additives, oxygenated organic compounds have emerged as highly effective modifiers for aqueous electrolytes, leveraging distinct hydrogen-bonding interactions to enhance low-temperature performance. Among these, dimethyl sulfoxide (DMSO) exemplifies this approach through its sulfoxide (S═O) functional group. The highly polar S═O moiety acts as a hydrogen-bond acceptor, forming robust interactions (S═O···H–O) with water's hydroxyl groups, thereby disrupting the native tetrahedral hydrogen-bonding network and suppressing ice crystallization.[8,11,111–113]

Molecular dynamics simulations by Nian *et al.* revealed a localized solvation structure featuring a 1 DMSO : 2H_2O molecular arrangement (Fig. 6F), which effectively depresses the electrolyte's freezing point to −50 °C.[81] The practical impact of this molecular-level engineering was demonstrated in a $NaTi_2(PO_4)_3$/C full cell using a 2 M LiTFSI-0.3DMSO electrolyte, which exhibited exceptional cycling stability at −50 °C. DMSO's benefits extend across diverse aqueous battery chemistries: sodium-ion batteries (NTP||AC) retained 61% of their room-temperature capacity (68 mAh g^{-1}) at −50 °C, while lithium-ion (LTP||AC) and potassium-ion (PI||AC) systems, previously inoperable at such temperatures, achieved 62% capacity retention.[81] These results establish oxygenated compounds like DMSO as a cornerstone strategy for enabling cryogenic aqueous battery operation through S═O-mediated hydrogen bonding disruption.

Hydroxyl-containing compounds leverage multiple –OH groups to achieve synergistic effects in hydrogen bonding disruption and ion coordination.[27,35,52,67,73,100,108,114,115] Ethylene glycol (EG) exemplifies this approach in zinc-based systems, where its multiple hydroxyl groups establish intricate hydrogen-bonding networks that become reinforced through Zn^{2+}-EG coordination upon $ZnSO_4$ introduction (Fig. 6J). Raman

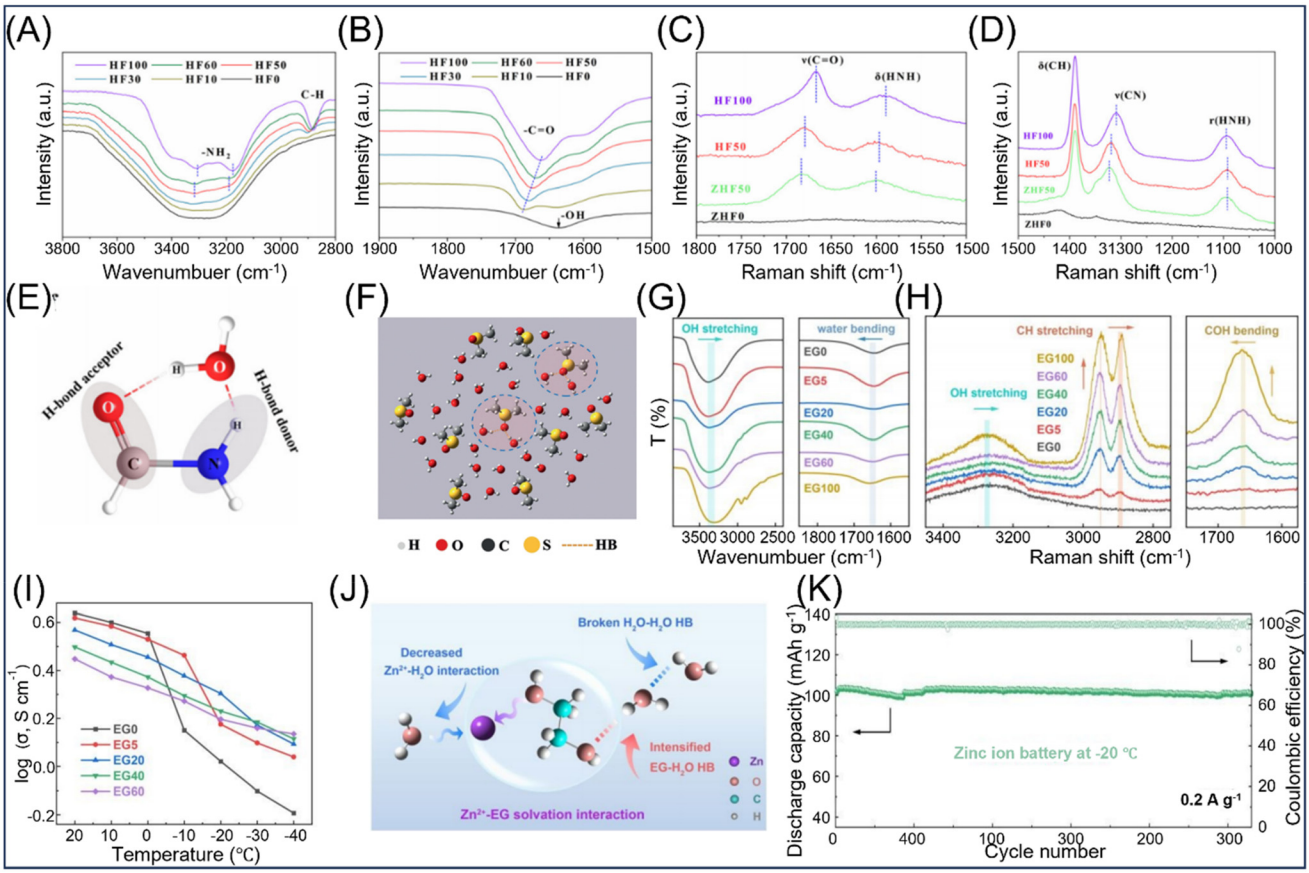

Fig. 6 (A) and (B) FTIR results of the mixture with different volume ratios between H_2O and FA (the mixture denoted as HF*x*, with *x* representing a volume fraction of *x*% for FA). (C) and (D) Raman results of the mixture with different volume ratios between H_2O and FA. (E) Schematic representation of the ring structure of FA–H_2O complexes. Reproduced from ref. 26 with permission from Royal Society of Chemistry, copyright 2023. (F) Schematic of the local structure of the cDMSO = 0.3 system in MD simulations. Reproduced from ref. 7 with permission from Wiley-VCH, copyright 2019. (G) FTIR results of the mixture with different volume ratios between H_2O and EG (the mixture denoted as EG*x*, with *x* representing a volume fraction of *x*% for EG). (H) Raman results of the mixture with different volume ratios between H_2O and EG. (I) Ionic conductivities of hybrid electrolytes at different temperatures. (J) Schematic diagram of EG affecting the electrolyte. (K) Cycling performance of EG40-based Zn//PANI-V_2O_5 cells at 0.2 A g^{-1} and −20 °C. Reproduced from ref. 52 with permission from Royal Society of Chemistry, copyright 2020.

spectroscopic analysis (Fig. 6G and H) reveals that this dual interaction simultaneously disrupts native water–water hydrogen bonding while facilitating ionic migration, effectively counteracting the viscosity increase typically induced by organic additives.[52] The optimized EG40 system maintains exceptional ionic conductivity (6.9 mS cm^{-1} at −40 °C, Fig. 6I) and delivers outstanding performance in Zn//PANI/V_2O_5 cells with 100 mAh g^{-1} capacity through 250 cycles at −20 °C (Fig. 6K).[52]

Saccharide-derived compounds further demonstrate the potential of hydroxyl-rich additives to achieve remarkable effects at minimal concentrations. The αDG additive, featuring five hydroxyl groups and one aldehyde group within its cyclic structure, exemplifies this efficiency. Bu *et al.* showed that αDG significantly reduces free water content while altering Zn^{2+} solvation environments through competitive coordination, additionally forming protective adsorption layers on zinc anodes (Fig. 7A and B).[74] Notably, αDG achieves optimal performance with minimal viscosity increase, depressing the freezing point to −55.3 °C and enabling stable cycling: 800 hours at −40 °C (5 mA cm^{-2}) and 10 000 cycles at −50 °C (Fig. 7C). These examples demonstrate how hydroxyl-rich compounds achieve superior low-temperature performance through coordinated molecular interactions at remarkably low additive concentrations.[74]

Beyond conventional polar additives, innovative design strategies have emerged to optimize low-temperature performance through hierarchical solvation engineering. Dong *et al.* demonstrated this concept by developing a biomimetic core–shell electrolyte system incorporating 1,2-dimethoxyethane (DME) into 1 M $Zn(OTf)_2$ aqueous solution (Fig. 7F). This architecture exploits DME's inherent low freezing point (−69 °C) while avoiding interference with Zn^{2+} coordination through controlled concentrations (Fig. 7E). The system operates *via* complementary mechanisms: OTf^- anions facilitate protective SEI formation that isolates water from reactive zinc surfaces, while DME's weakly polar ether groups disrupt bulk water hydrogen bonding, suppressing crystallization to

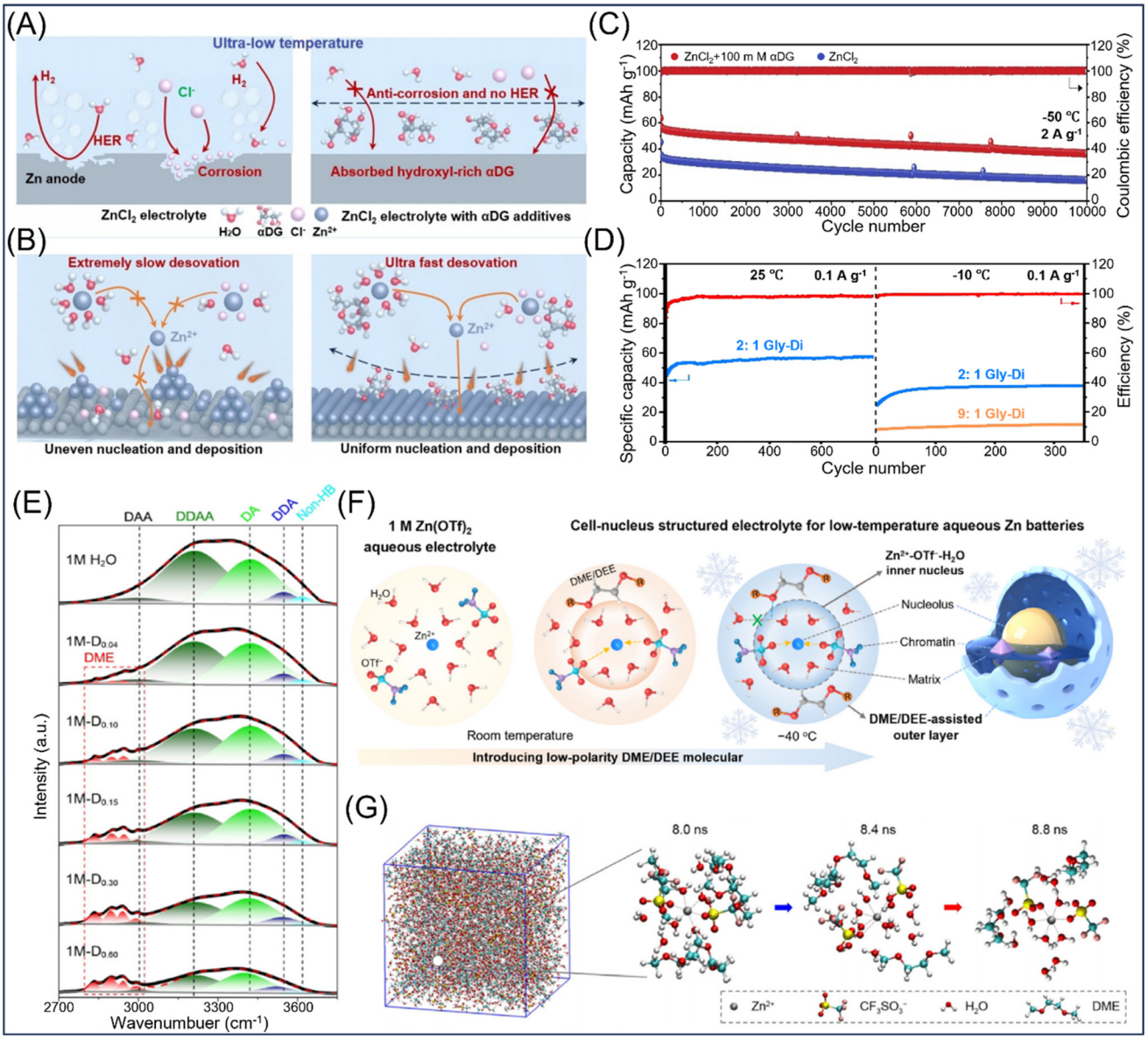

Fig. 7 (A) and (B) Schematic mechanism of $ZnCl_2$ and mimetic $ZnCl_2$-αDG electrolytes with zinc negative electrode at low temperature. (C) Cycling performance of EG40-based Zn//PANI cells at 2 A g^{-1} under −50 °C. Reproduced from ref. 74 with permission from Wiley-VCH, copyright 2024. (D) Cycling performance of Ni_2ZnHCF||PTCDI cells at −20 °C and 25 °C at 0.1 A g^{-1}. Reproduced from ref. 109 with permission from Wiley-VCH, copyright 2022. (E) FTIR spectra of 1 M-D_x electrolytes (the mixture denoted as 1 M-D_x, x is the molar ratio of DME to DME + H_2O (M_{DME})). (F) Schematic design of the core-structured electrolyte of a cell with a low dose of DME/DEE additive introduced into 1 M $Zn(OTf)_2$ aqueous solution electrolyte. (G) Snapshots of 1 M-$D_{0.15}$ and the conformational evolution of the bilayer Zn^{2+} solvation structure at 8.0, 8.4, and 8.8 ns. Reproduced from ref. 28 with permission from Elsevier, copyright 2023.

−52.4 °C. Molecular dynamics simulations reveal dynamic Zn^{2+} coordination shifts during charge transfer (Fig. 7G), with the optimized electrolyte achieving 1.06 mS cm^{-1} conductivity at −40 °C and 81% capacity retention over 1050 cycles.[28]

Multi-functional organic additives represent another advanced approach, simultaneously addressing multiple battery challenges beyond temperature stability. Sun *et al.* demonstrated this concept using glycerol in sodium-based systems, where the additive not only enables low-temperature operation through hydrogen bonding disruption but also extends the electrochemical stability window to 2.7 V.[109] This dual functionality delivered 40 mAh g^{-1} capacity at −10 °C in Ni_2ZnHCF||PTCDI cells with stable cycling (Fig. 7D), illustrating how rational molecular design can address the inherent limitations of aqueous systems through coordinated property optimization.[109]

The development of organic additives for low-temperature aqueous batteries demonstrates systematic progress from simple polar molecules to sophisticated multi-functional systems, successfully expanding the practical temperature

window to −55 °C while maintaining impressive performance metrics.[74] The evolution from single-function additives like formamide to bio-inspired hierarchical structures and multi-functional designs has established diverse approaches for modifying both bulk electrolyte properties and interfacial stability.[28] The successful implementation across various battery chemistries (Zn-, Na-, and Li-based systems) highlights the versatility of organic additives in regulating hydrogen bonding networks and controlling ion solvation structures.[102,110,116–119] Future developments may focus on rational design of multi-functional molecules, understanding synergistic effects between different functional groups, and establishing predictive models for optimal additive selection based on molecular features and battery chemistry requirements. Environmental considerations are increasingly important in additive selection, with bio-based compounds like ethylene glycol and saccharides offering superior biodegradability compared to synthetic alternatives (detailed analysis in Section 4.2).

3.4 Gel electrolyte architectures

While additive-based strategies have significantly improved low-temperature aqueous batteries, traditional liquid electrolytes continue to face fundamental limitations under freezing

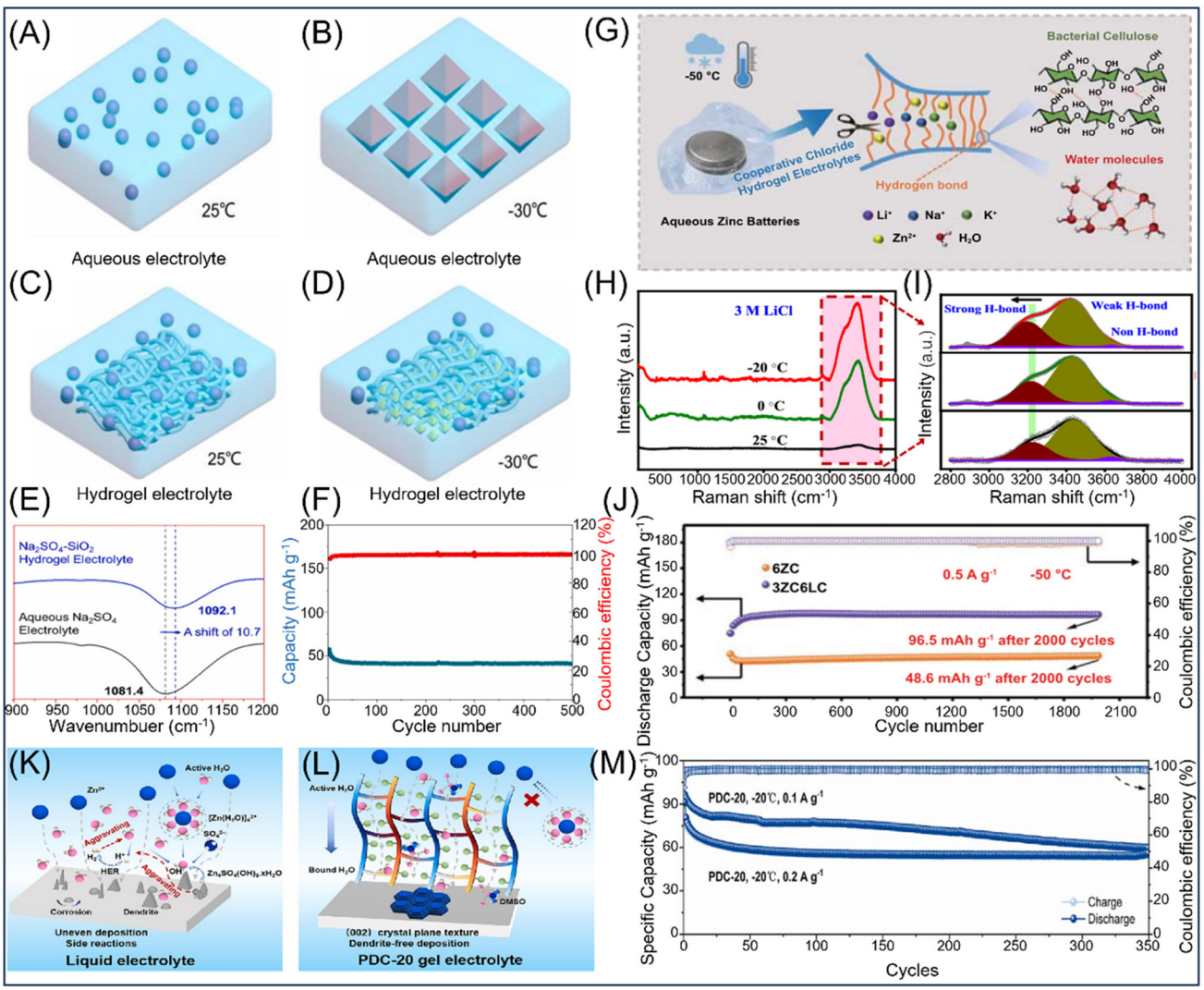

Fig. 8 (A)–(D) Illustration of freezing process at 25 °C and −30 °C for aqueous Na_2SO_4 electrolytes and Na_2SO_4–SiO_2 hydrogel electrolytes. (E) FTIR results of the triply degenerate symmetric stretching mode of SO_4^{2-} in aqueous Na_2SO_4 electrolyte and Na_2SO_4–SiO_2 hydrogel electrolyte. (F) Cycling performance of $NaTi_2(PO_4)_3$@C||$LiMn_2O_4$ ells at 1C (1C = 0.13 A g^{-1}) under −30 °C. Reproduced from ref. 115 with permission from Elsevier, copyright 2021. (G) Schematic diagram of interrupted H-bonds between cellulose and cellulose chains, water and water molecules induced by cations (Li^+, Na^+, and K^+) at low temperature. (H) and (I) Raman spectra of 3 M LiCl hydrogel electrolytes and fitted O–H stretching vibrations represent electrolytes with strong, weak, and non-H-bonds. (J) Cycling performance of Zn||$LiFePO_4$ cells at 0.2 A g^{-1} under −20 °C. Reproduced from ref. 82 with permission from Wiley-VCH, copyright 2022. (K) and (L) Illustration of Zn deposition process and interfacial reaction mechanism with aqueous electrolyte and PDC-20 hydrogel electrolytes. (M) Cycling performance of Zn||MnO_2@CNT cells at 0.1 A g^{-1} and 0.2 A g^{-1} under −20 °C with PDC-20 gel electrolyte. Reproduced from ref. 10 with permission from Springer Singapore, copyright 2023.

conditions, including electrolyte crystallization, dramatic conductivity drops, and disruptive volumetric changes.[120–122] Hydrogel electrolytes have emerged as a transformative solution to overcome these constraints through their innovative three-dimensional polymer network architecture. These systems leverage interconnected hydrophilic polymer networks within aqueous environments to deliver critical performance enhancements: maintained ionic conductivity under subzero temperatures, exceptional mechanical flexibility with preserved structural integrity, and effective suppression of ice nucleation and dendrite growth.[123,124] Unlike liquid systems that rely solely on molecular modifications, gel electrolytes provide both physical constraints through polymer networks and chemical optimization through functional group interactions, enabling comprehensive solutions for extreme-temperature operation.[125–127]

The superior performance of gel electrolytes stems from synergistic mechanisms operating at multiple scales. The polymer network architecture physically restricts ice nucleation and crystalline propagation, while functional groups along polymer chains (hydroxyl, ester, carbonyl) actively disrupt water's hydrogen bonding network.[128–130] Metal ion coordination with these functional groups reshapes solvation environments and excludes reactive water molecules, simultaneously facilitating ion transport and suppressing parasitic reactions. Additionally, the crosslinked matrix accommodates strategic integration of low-temperature additives, creating optimized microenvironments that enhance both bulk electrolyte properties and interfacial stability. This multi-mechanism approach enables gel electrolytes to maintain electrochemical functionality while providing mechanical robustness under extreme thermal conditions.[15,28,37] In Table S3, we summarize the data regarding the improvement of battery performance through the use of gel electrolytes at low temperatures.

The effectiveness of gel electrolyte design principles has been demonstrated through several representative systems with distinct optimization strategies. Cheng *et al.* developed a composite gel combining fumed silica with sodium sulfate and methanol, where the silica framework physically restricts ice crystal expansion while methanol provides antifreeze effects (Fig. 8A–D). Achieving stable operation at −30 °C with 61.8 mAh g^{-1} capacity (Fig. 8E and F).[115] Yan *et al.* advanced this concept using bacterial cellulose hydrogel with dual salts (3 M $ZnCl_2$ + 6 M LiCl), strategically applying Hofmeister effects to minimize water activity and achieve exceptional metrics: 1.14 mS cm^{-1} conductivity and 0.21 eV activation energy at −50 °C (Fig. 8G–J).[82] Huang *et al.* further pushed molecular engineering boundaries by developing DMSO-functionalized 3D networks that establish three-way hydrogen bonding among polymer chains, water, and additives, delivering 151.8 mAh g^{-1} at −20 °C while maintaining 1.52 mS cm^{-1} conductivity at −30 °C (Fig. 8K–M). These examples demonstrate the evolution from simple physical constraints to sophisticated molecular-level engineering for optimized low-temperature performance.[10]

The development of gel electrolyte systems represents a significant advancement in low-temperature aqueous battery technology, demonstrating systematic progress from simple polymer networks to sophisticated multi-component designs. These systems have successfully expanded the practical temperature window to −50 °C while maintaining key performance metrics including high ionic conductivity (>1 mS cm^{-1}) and stable cycling performance.[82] The synergistic integration of network structures, functional groups, and strategic additives provides multiple mechanisms for freezing point depression and performance enhancement, with particular success in zinc-based systems highlighting their potential for next-generation energy storage applications.[115] Future developments may focus on molecular-level design of functional polymer networks, understanding complex multi-component interactions, and establishing predictive models for optimal gel electrolyte formulation. Additionally, exploring bio-inspired architectures and developing scalable synthesis methods will be crucial for translating laboratory achievements to practical applications.

4 Conclusion and perspective

4.1 Summary and conclusions

This comprehensive review has systematically examined electrolyte modification strategies for low-temperature aqueous batteries, revealing fundamental principles that govern performance enhancement across extreme temperature ranges. Through detailed analysis of concentration engineering, inorganic additives, organic additives, and gel electrolyte architectures, we have established that successful low-temperature operation requires strategic disruption of water's hydrogen bonding network while maintaining favorable ion transport properties. The diverse modification approaches demonstrate remarkable versatility in overcoming traditional aqueous system limitations, with concentration engineering achieving operation down to −70 °C through higher concentration configurations, inorganic additives enabling stable cycling at −60 °C *via* structure-breaking mechanisms, organic additives providing multi-functional enhancement to −55 °C through coordinated solvation engineering, and gel electrolytes delivering robust performance at −50 °C through synergistic polymer-additive interactions.[26,71,115]

The systematic examination of modification strategies has revealed several unifying principles that transcend individual approaches and provide a theoretical foundation for rational electrolyte design. The multi-scale synergistic regulation theory emerges as a central paradigm, demonstrating that optimal low-temperature performance requires coordinated interventions across molecular solvation environments, interfacial charge transfer processes, and bulk transport properties. This framework explains why hybrid strategies consistently outperform single-component modifications.[131–133] The synergistic interactions between these mechanisms create emergent behaviors that cannot be predicted from individual component

analysis, establishing clear structure–property relationships that guide systematic optimization.[25,32,107]

Advanced characterization techniques offer unprecedented insights into the molecular mechanisms behind performance improvements, showing how strategies target water structure and ion coordination. Synchrotron-based methods like XAFS analyze atomic valence and coordination in electrodes, SAXS captures nanostructural changes, and XRD tracks crystal structure variations. Spectroscopic techniques such as Raman and FTIR detect hydrogen bonding and functional group interactions, while NMR provides ion solvation dynamics. Electrochemical methods like cyclic voltammetry and impedance spectroscopy correlate additives with battery performance, validating mechanistic hypotheses.[98,134,135]

4.2 Sustainability considerations and future research directions

While the preceding analysis has demonstrated significant progress in electrolyte modification strategies, the practical implementation of low-temperature aqueous batteries requires addressing two critical considerations, which are environmental sustainability and remaining technical challenges. This section evaluates the environmental impact of different modification approaches and identifies key research directions needed to advance the field toward commercial viability.

The environmental and safety characteristics of different chemical substances significantly impact sustainable low-temperature aqueous battery design. Table S4 provides comprehensive safety data revealing substantial performance differences among various additives. Biodegradability assessment shows dramatic variations: environmentally compatible materials ($Zn(OAc)_2$ >99%, ethylene glycol >90%, propylene glycol >99%) demonstrate excellent degradation within 28 days, while problematic additives (LiTFSI <5%, perfluoropolyethers <1%, $LiPF_6$ non-biodegradable) exhibit poor degradation leading to environmental accumulation. Production energy consumption varies eight-fold, from efficient $Zn(OAc)_2$ (12–18 MJ kg^{-1}) to energy-intensive LiTFSI (120–150 MJ kg^{-1}) and perfluoropolyethers (180–220 MJ kg^{-1}). Toxicity profiles range from near non-toxic (ethylene glycol) to moderate acute toxicity requiring specific safety protocols.

Perfluorinated compounds present critical environmental concerns due to strong carbon–fluorine bonds, which resist biological degradation processes, high bioaccumulation potential, and environmental persistence. Despite their electrochemical advantages, these materials are incompatible with sustainable battery design principles. Bioaccumulation risk assessment reveals that perfluorinated solvents persist in biological systems, potentially causing long-term ecological damage, while bio-based additives undergo natural degradation pathways. The quantitative framework demonstrates that sustainable low-temperature battery development requires balancing electrochemical performance with environmental compatibility. High-performing, environmentally responsible solutions are both feasible and essential for green energy storage technologies.

However, several critical knowledge gaps limit our ability to fully exploit the potential of low-temperature aqueous batteries and represent the most pressing scientific challenges for future research (Fig. 9). The formation and evolution of SEI during freeze–thaw cycles present significant characterization challenges that current techniques struggle to address comprehensively. Spatial and temporal resolution constraints pose fundamental challenges, as SEI layers exist at nanometer scales while freeze–thaw cycles occur over minutes to hours, requiring simultaneous high resolution that exceeds current capabilities. Environmental interference severely impacts data quality: ice crystal formation creates optical artifacts in microscopy, water's strong Raman background obscures SEI signals, and aqueous environments prevent vacuum-based

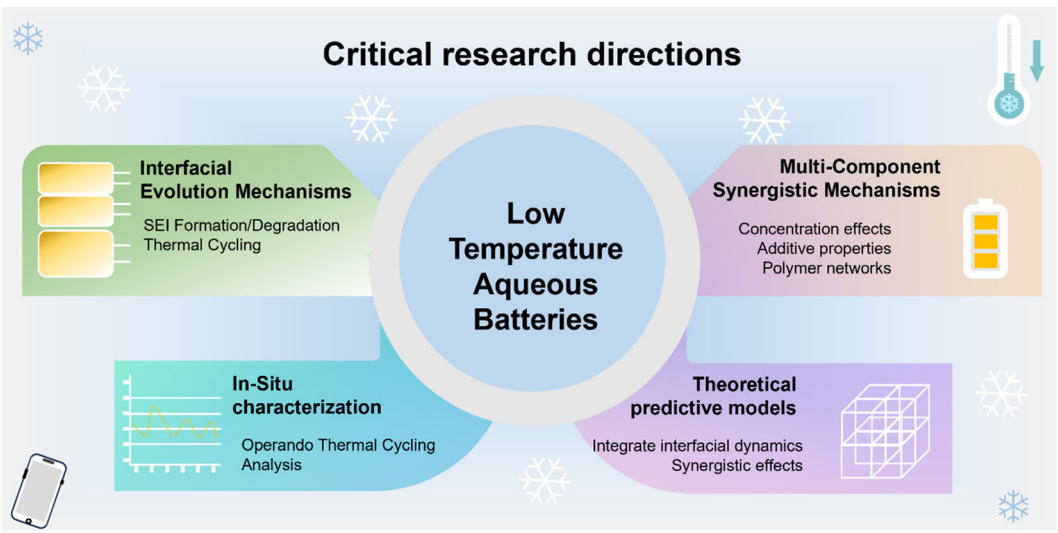

Fig. 9 Schematic diagram of research directions for low-temperature water-based batteries.

techniques like XPS from operating under realistic conditions. Sample preparation limitations further complicate analysis, as cryogenic preparation can introduce structural artifacts while the dynamic nature of freeze–thaw processes makes *ex situ* analysis inadequate for capturing transient states.

Technique-specific constraints add additional barriers, where TEM suffers from electron beam damage and ice interference; AFM faces probe-ice interactions reducing resolution; NMR experiences signal reduction at low temperatures; and synchrotron techniques require specialized environments with limited accessibility. Most critically, multi-scale complexity represents the greatest challenge, as SEI evolution involves simultaneous molecular-level chemistry, nanoscale structure changes, and microscale mechanical stress—processes no single technique can capture comprehensively. These limitations collectively explain why SEI evolution mechanisms during freeze–thaw cycles remain poorly understood, highlighting the need for advanced characterization approaches to address these fundamental challenges.

The complex interplay between bulk electrolyte modifications and temperature-dependent interfacial processes requires systematic investigation to enable long-term performance prediction. Multi-component synergistic optimization represents another challenge, as the mechanisms governing interactions between different modification strategies remain largely empirical. While combination approaches consistently outperform single modifications, rational design principles for optimal formulations are still lacking. Based on these fundamental challenges, several critical research directions emerge:

1. Investigation of interfacial evolution mechanisms through systematic study of SEI formation and degradation during thermal cycling, establishing fundamental understanding of temperature-dependent interfacial processes across different modification strategies.

2. Elucidation of multi-component synergistic mechanisms through comprehensive analysis of interactions between concentration effects, additive properties, and polymer networks, enabling rational prediction of optimal combinations rather than empirical screening.

3. Development of advanced *in situ* characterization techniques capable of real-time monitoring of both interfacial changes and bulk electrolyte behavior during thermal cycling under realistic operating conditions, providing essential tools for mechanistic understanding.

4. Establishment of theoretical predictive models that integrate interfacial dynamics and synergistic effects to enable rational electrolyte design, accelerating the transition from laboratory demonstrations to practical applications.

Addressing these research priorities will be essential for translating the fundamental insights gained from electrolyte modification strategies into practical low-temperature aqueous battery technologies. The integration of sustainable materials selection with advanced characterization capabilities and theoretical modeling will enable the rational design of next-generation electrolyte systems that meet both performance and environmental requirements for extreme-condition applications.

Conflicts of interest

The authors declare no competing financial interest.

Data availability

The data supporting this article has been included as part of the SI. The Supplementary Information includes detailed performance comparison tables for different battery electrolyte systems (Tables S1–S3), material safety data sheets and environmental assessments for recycling chemicals (Table S4), and cost analysis for common battery electrolyte solutions (Figure S1). These materials provide supporting data for the performance evaluations, safety considerations, and economic analyses discussed in the main text. See DOI: **https://doi.org/10.1039/d5gc02967h**.

Acknowledgements

This work was funded by the Startup fund at Hubei University of Technology (Grant No. 00709, 00843 and 00967), and a High-level Talent grant from Hubei Province (Grant No. GCC2024012).

References

1 G. Yang, J. Huang, X. Wan, B. Liu, Y. Zhu, J. Wang, O. Fontaine, S. Luo, P. Hiralal, Y. Guo and H. Zhou, *EcoMat*, 2022, **4**, 1–11.
2 L. Jiang, Y. Lu, C. Zhao, L. Liu, J. Zhang, Q. Zhang, X. Shen, J. Zhao, X. Yu, H. Li, X. Huang, L. Chen and Y. S. Hu, *Nat. Energy*, 2019, **4**, 495–503.
3 H. Wang, H. Zhang, Y. Cheng, K. Feng, X. Li and H. Zhang, *Electrochim. Acta*, 2018, **278**, 279–289.
4 K. Zhu, Z. Sun, T. Jin, X. Chen, Y. Si, H. Li and L. Jiao, *Batteries Supercaps*, 2022, **5**, e202200308.
5 Z. Zhao, Z. Zhang, T. Xu, W. Wang, B. Wang and X. Yu, *J. Am. Chem. Soc.*, 2024, **146**, 2257–2266.
6 Z. Hao, J. Wang, J. Feng, Y. Fan, J. Peng, J. Wang and S. Dou, *Carbon Energy*, 2025, **7**, e681.
7 Q. Nian, J. Wang, S. Liu, T. Sun, S. Zheng, Y. Zhang, Z. Tao and J. Chen, *Angew. Chem., Int. Ed.*, 2019, **58**, 16994–16999.
8 D. Feng, F. Cao, L. Hou, T. Li, Y. Jiao and P. Wu, *Small*, 2021, **17**, 1–11.
9 Y. He, W. Shang and P. Tan, *Carbon Neutralization*, 2024, **3**, 773–780.
10 S. Huang, S. He, Y. Li, S. Wang and X. Hou, *Chem. Eng. J.*, 2023, **464**, 142607.
11 B. Hu, M. Wang, P. Lu, L. Yu, H. Li, Z. Rao, S. Bian, K. Liu and M. Zhang, *J. Energy Chem.*, 2025, **106**, 742–750.
12 Q. Zhao, Y. Wu, Z. Yang, D. Song, X. Sun, C. Wang, L. Yang, Y. Zhang, J. Gao, T. Ohsaka, F. Matsumoto and J. Wu, *Chem. Eng. J.*, 2022, **440**, 135939.

13 S. Kim, J. Jung, I. Kim, H. Kwon, H. Cho and H. T. Kim, *Energy Storage Mater.*, 2023, **59**, 102763.
14 W. Lv, C. Zhu, J. Chen, C. Ou, Q. Zhang and S. Zhong, *Chem. Eng. J.*, 2021, **418**, 129400.
15 C. Liu, Z. Li, L. Jiang, H. Zhu, F. Wang and L. Sheng, *J. Energy Chem.*, 2025, **104**, 678–686.
16 C. M. Paleos and D. Tsiourvas, *Adv. Mater.*, 1997, **9**, 695–710.
17 J. Hao, L. Yuan, C. Ye, D. Chao, K. Davey, Z. Guo and S. Z. Qiao, *Angew. Chem., Int. Ed.*, 2021, **60**, 7366–7375.
18 G. C. Sosso, J. Chen, S. J. Cox, M. Fitzner, P. Pedevilla, A. Zen and A. Michaelides, *Chem. Rev.*, 2016, **116**, 7078–7116.
19 E. B. Moore and V. Molinero, *Nature*, 2011, **479**, 506–508.
20 C. Zhu, J. Zhou, Z. Wang, Y. Zhou, X. He, X. Zhou, J. Liu, C. Yan and T. Qian, *Chem. Eng. J.*, 2023, **454**, 140413.
21 X. Rao, Y. Han, L. Luo, L. Hu, L. Yan, B. Xiang, Y. Zhou and X. Zou, *Energy Storage Mater.*, 2025, **79**, 104326.
22 C. You, W. Fan, X. Xiong, H. Yang, L. Fu, T. Wang, F. Wang, Z. Zhu, J. He and Y. Wu, *Adv. Funct. Mater.*, 2024, **34**, 2403616.
23 G. Liu, L. Hu, Y. Liu, M. Xu, J. Guo, H. Zhou, G. Ma, H. Lin, Z. Su, C. Liu, J. Zhao, C. Dai and Z. Lin, *Energy Environ. Sci.*, 2025, **18**, 6180–6190.
24 Y. Zheng, T. Qian, J. Zhou, J. Liu, Z. Wang, S. Wang, Y. Wang and C. Yan, *Adv. Energy Mater.*, 2023, **13**, 1–28.
25 Y. Pu, C. Wang, J. Feng, Y. Xu, K. Su, B. Yang, G. Tian and J. Lang, *J. Power Sources*, 2023, **571**, 233061.
26 C. You, R. Wu, X. Yuan, L. Liu, J. Ye, L. Fu, P. Han and Y. Wu, *Energy Environ. Sci.*, 2023, **16**, 5096–5107.
27 T. Nguyen Thanh Tran, M. Zhao, S. Geng and D. G. Ivey, *Batteries Supercaps*, 2022, **5**, 1–8.
28 Y. Dong, N. Zhang, Z. Wang, J. Li, Y. Ni, H. Hu and F. Cheng, *J. Energy Chem.*, 2023, **83**, 324–332.
29 Q. Zhang, Y. Ma, Y. Lu, L. Li, F. Wan, K. Zhang and J. Chen, *Nat. Commun.*, 2020, **11**, 1–10.
30 Y. Lin, Z. Yang, X. Zhang, Y. Liu, G. Hu, S. Chen and Y. Zhang, *Energy Storage Mater.*, 2023, **58**, 184–194.
31 G. Yang, X. Xu, G. Qu, J. Deng, Y. Zhu, C. Fang, O. Fontaine, P. Hiralal, J. Zheng and H. Zhou, *Chem. Eng. J.*, 2023, **455**, 140806.
32 Y. Cheng, X. Chi, J. Yang and Y. Liu, *J. Energy Storage*, 2021, **40**, 102701.
33 L. Suo, O. Borodin, W. Sun, X. Fan, C. Yang, F. Wang, T. Gao, Z. Ma, M. Schroeder, A. von Cresce, S. M. Russell, M. Armand, A. Angell, K. Xu and C. Wang, *Angew. Chem., Int. Ed.*, 2016, **55**, 7136–7141.
34 J. Wang, Q. Zhu, F. Li, J. Chen, H. Yuan, Y. Li, P. Hu, M. S. Kurbanov and H. Wang, *Chem. Eng. J.*, 2022, **433**, 134589.
35 A. Tron, S. Jeong, Y. D. Park and J. Mun, *ACS Sustainable Chem. Eng.*, 2019, **7**, 14531–14538.
36 W. Yang, X. Du, J. Zhao, Z. Chen, J. Li, J. Xie, Y. Zhang, Z. Cui, Q. Kong, Z. Zhao, C. Wang, Q. Zhang and G. Cui, *Joule*, 2020, **4**, 1557–1574.
37 Z. Zhu, H. Ma, H. Du, L. Zhang, J. Wu, C. Gao, W. Li, X. Chen, Y. Su, D. Wang, X. Chen and Z. He, *Angew. Chem., Int. Ed.*, 2025, **64**, e202505325.
38 D. T. Hickson, J. Im, D. M. Halat, A. Karvat, J. A. Reimer and N. P. Balsara, *J. Electrochem. Soc.*, 2024, **171**, 030514.
39 Y. Dong, H. Hu, P. Liang, L. Xue, X. Chai, F. Liu, M. Yu and F. Cheng, *Nat. Rev. Chem.*, 2025, **9**, 102–117.
40 T. Sun, S. Zheng, H. Du and Z. Tao, *Nano-Micro Lett.*, 2021, **13**, 1–10.
41 L. Jiang, S. Han, Y. C. Hu, Y. Yang, Y. Lu, Y. C. Lu, J. Zhao, L. Chen and Y. S. Hu, *Nat. Energy*, 2024, **9**, 839–848.
42 R. Wang, Q. Ma, L. Zhang, Z. Liu, J. Wan, J. Mao, H. Li, S. Zhang, J. Hao, L. Zhang and C. Zhang, *Adv. Energy Mater.*, 2023, **13**, 2302543.
43 M. Alahmadi, E. El-Dek, M. A. Moselhy, A. M. Mostafa, S. H. Neair, H. S. Refai, M. M. El-Desoky, X. Y. Yang and E. Sheha, *J. Solid State Electrochem.*, 2024, **28**, 3109–3122.
44 Z. Liu, M. Xi, R. Sheng, Y. Huang, J. Ding, Z. Tan, J. Li, W. Zhang and Y. Wang, *Nano-Micro Lett.*, 2025, **17**, 120.
45 J. Sun, Y. Yao, X. Cui, J. Luo, J. Zhang, Y. Zhao, H. Wang, J. Zhou, J. Zhu, Y. Wang, C. Li, N. Zhang, L. Zhang, S. Li and D. Zhao, *Battery Energy*, 2025, **4**, e20240106.
46 A. Ramanujapuram and G. Yushin, *Adv. Energy Mater.*, 2018, **8**, 1–8.
47 S. Boon-In, M. Theerasilp and D. Crespy, *ACS Appl. Polym. Mater.*, 2023, **5**, 2562–2574.
48 T. Sun, C. Liu, J. Wang, Q. Nian, Y. Feng, Y. Zhang, Z. Tao and J. Chen, *Nano Res.*, 2020, **13**, 676–683.
49 Y. Sun, B. Liu, L. Liu, J. Lang and J. Qiu, *Small Struct.*, 2023, **4**, 1–9.
50 C. Lin, X. Yang, P. Xiong, H. Lin, L. He, Q. Yao, M. Wei, Q. Qian, Q. Chen and L. Zeng, *Adv. Sci.*, 2022, **9**, 1–10.
51 Q. Nian, T. Sun, S. Liu, H. Du, X. Ren and Z. Tao, *Chem. Eng. J.*, 2021, **423**, 130253.
52 N. Chang, T. Li, R. Li, S. Wang, Y. Yin, H. Zhang and X. Li, *Energy Environ. Sci.*, 2020, **13**, 3527–3535.
53 K. Zhu, Z. Li, Z. Sun, P. Liu, T. Jin, X. Chen, H. Li, W. Lu and L. Jiao, *Small*, 2022, **18**, 1–8.
54 M. Zhu, X. Wang, H. Tang, J. Wang, Q. Hao, L. Liu, Y. Li, K. Zhang and O. G. Schmidt, *Adv. Funct. Mater.*, 2020, **30**, 1–10.
55 H. Wang, T. Liu, X. Du, J. Wang, Y. Yang, H. Qiu, G. Lu, H. Li, Z. Chen, J. Zhao and G. Cui, *Batteries Supercaps*, 2022, **5**, 1–8.
56 X. Wang, H. Huang, F. Zhou, P. Das, P. Wen, S. Zheng, P. Lu, Y. Yu and Z. S. Wu, *Nano Energy*, 2021, **82**, 105688.
57 C. Yang, J. Xia, C. Cui, T. P. Pollard, J. Vatamanu, A. Faraone, J. A. Dura, M. Tyagi, A. Kattan, E. Thimsen, J. Xu, W. Song, E. Hu, X. Ji, S. Hou, X. Zhang, M. S. Ding, S. Hwang, D. Su, Y. Ren, X. Q. Yang, H. Wang, O. Borodin and C. Wang, *Nat. Sustainable*, 2023, **6**, 325–335.
58 Y. Pu, K. Su, C. Wang, Y. Wang, B. Yang, G. Tian, H. Du and J. Lang, *Electrochim. Acta*, 2024, **487**, 144179.
59 H. Huang, Z. Zhao, P. Li, H. Zhang and G. Li, *J. Power Sources*, 2024, **602**, 234340.

60 Y. Liu, T. J. Frankcombe and T. W. Schmidt, *J. Phys. Chem. Lett.*, 2020, **11**, 735–739.
61 R. Ludwig, *ChemPhysChem*, 2007, **8**, 938–943.
62 B. Han, C. M. Isborn and L. Shi, *J. Chem. Theory Comput.*, 2021, **17**, 889–901.
63 M. Qiu, P. Sun, Y. Liang, J. Chen, Z. L. Wang and W. Mai, *Nat. Commun.*, 2024, **15**, 1–10.
64 Q. Zhang, K. Xia, Y. Ma, Y. Lu, L. Li, J. Liang, S. Chou and J. Chen, *ACS Energy Lett.*, 2021, **6**, 2704–2712.
65 H. J. Jiang, T. C. Underwood, J. G. Bell, S. Ranjan, D. Sasselov and G. M. Whitesides, *Proc. Natl. Acad. Sci. U. S. A.*, 2017, **120**, 2017.
66 A. Oleinikova, I. Brovchenko, A. Geiger and B. Guillot, *J. Chem. Phys.*, 2002, **117**, 3296–3304.
67 T. Wei, Y. Peng, L. Mo, S. Chen, R. Ghadari, Z. Li and L. Hu, *Sci. China Mater.*, 2022, **65**, 1156–1164.
68 G. Bai, D. Gao, Z. Liu, X. Zhou and J. Wang, *Nature*, 2019, **576**, 437–441.
69 M. Qiu, P. Sun, K. Han, Z. Pang, J. Du, J. Li, J. Chen, Z. L. Wang and W. Mai, *Nat. Commun.*, 2023, **14**, 601.
70 M. Matsumoto, S. Saito and I. Ohmine, *Nature*, 2002, **416**, 409–413.
71 T. Sun, H. Du, S. Zheng, J. Shi and Z. Tao, *Adv. Funct. Mater.*, 2021, **31**, 1–7.
72 A. Saeed, S. F. A. Zaidi, J. Mun, H. K. Cho, S. B. Jung, N. E. Lee, C. G. Park and J. H. Lee, *J. Mater. Chem. C*, 2024, **12**, 6213–6225.
73 Y. Zhu, Q. Chen, J. Hao and Y. Jiao, *J. Mater. Chem. A*, 2024, **12**, 20097–20106.
74 F. Bu, Y. Gao, W. Zhao, Q. Cao, Y. Deng, J. Chen, J. Pu, J. Yang, Y. Wang, N. Yang, T. Meng, X. Liu and C. Guan, *Angew. Chem., Int. Ed.*, 2024, **63**, e202318496.
75 J. Feng, W. Zhou, Z. Chen and Z. Hao, *Nano Energy*, 2024, **119**, 109028.
76 R. Lv, Z. Chen, W. Zhou, L. Zhang, L. Sheng, P. Yao, F. R. Wang, Z. Hao and J. Feng, *Small*, 2024, **2406635**, 1–12.
77 T. Phusittananan, W. Kao-Ian, M. T. Nguyen, T. Yonezawa, R. Pornprasertsuk, A. A. Mohamad and S. Kheawhom, *Front. Energy Res.*, 2020, **8**, 1–12.
78 J. Yao, B. Zhang, X. Wang, L. Tao, J. Ji, Z. Wu, X. Liu, J. Li, Y. Gan, J. Zheng, L. Lv, X. Ji, H. Wang, J. Zhang, H. Wang and H. Wan, *Angew. Chem., Int. Ed.*, 2024, **63**, e202409986.
79 W. Wang, H. Yu, L. Ma, Y. Zhang, Y. Chen, L. Chen, G. Kuang, L. Zhou and W. Wei, *J. Power Sources*, 2024, **591**, 23384.
80 J. Nan, Y. Sun, F. Yang, Y. Zhang, Y. Li, Z. Wang, C. Wang, D. Wang, F. Chu, C. Wang, T. Zhu and J. Jiang, *Nano-Micro Lett.*, 2024, **16**, 1–17.
81 Q. Nian, J. Wang, S. Liu, T. Sun, S. Zheng, Y. Zhang, Z. Tao and J. Chen, *Angew. Chem.*, 2019, **131**, 17150–17155.
82 C. Yan, Y. Wang, X. Deng and Y. Xu, *Nano-Micro Lett.*, 2022, **14**, 1–15.
83 J. Yao, B. Zhang, X. Wang, L. Tao, J. Ji, Z. Wu, X. Liu, J. Li, Y. Gan, J. Zheng, L. Lv, X. Ji, H. Wang, J. Zhang, H. Wang and H. Wan, *Angew. Chem., Int. Ed.*, 2024, **63**, e202409986.
84 J. P. A. Santos, M. J. Pinzón, É.A Santos, R. Vicentini, C. J. B. Pagan, L. M. Da Silva and H. Zanin, *J. Energy Chem.*, 2022, **70**, 521–530.
85 H. Dong, S. Yan, T. Li, K. Ming, Y. Zheng, Z. Liu, G. Li, J. Liu, H. Li, Q. Wang, X. Hua and Y. Wang, *J. Power Sources*, 2023, **585**, 233593.
86 G. Su, S. Chen, H. Dong, Y. Cheng, Q. Liu, H. Wei, E. H. Ang, H. Geng and C. C. Li, *Nanoscale*, 2021, **13**, 2399–2407.
87 C. Knight and G. A. Voth, *Acc. Chem. Res.*, 2012, **45**, 101–109.
88 B. Hao, J. Zhou, H. Yang, C. Zhu, Z. Wang, J. Liu, C. Yan and T. Qian, *Nat. Commun.*, 2024, **15**, 9465.
89 J. Chen, J. Vatamanu, L. Xing, O. Borodin, H. Chen, X. Guan, X. Liu, K. Xu and W. Li, *Adv. Energy Mater.*, 2020, **10**, 1–10.
90 Y. Lin, Z. Yang, X. Zhang, Y. Liu, G. Hu, S. Chen and Y. Zhang, *Energy Storage Mater.*, 2023, **58**, 184–194.
91 L. Suo, O. Borodin, T. Gao, M. Olguin, J. Ho, X. Fan, C. Luo, C. Wang and K. Xu, *Science*, 2015, **350**, 938–943.
92 X. Yuan, D. Zhang, H. Lu, C. Duan and Y. Jin, *IET Energy Syst. Integr.*, 2024, **6**, 702–723.
93 H. Ao, C. Chen, Z. Hou, W. Cai, M. Liu, Y. Jin, X. Zhang, Y. Zhu and Y. Qian, *J. Mater. Chem. A*, 2020, **8**, 14190–14197.
94 M. H. Lee, S. J. Kim, D. Chang, J. Kim, S. Moon, K. Oh, K. Y. Park, W. M. Seong, H. Park, G. Kwon, B. Lee and K. Kang, *Mater. Today*, 2019, **29**, 26–36.
95 F. Yin, Z. Liu, S. Yang, Z. Shan, Y. Zhao, Y. Feng, C. Zhang and Z. Bakenov, *Nanoscale Res. Lett.*, 2017, **12**, 1–9.
96 Y. Zhang, Z. Bakenov, T. Tan and J. Huang, *Polymers*, 2018, **10**, 853.
97 X. Zhang, R. Wang, Z. Liu, Q. Ma, H. Li, Y. Liu, J. Hao, S. Zhang, J. Mao and C. Zhang, *Adv. Energy Mater.*, 2024, **14**, 1–13.
98 X. Yang, Y. Zhang, M. Ye, Y. Tang, Z. Wen, X. Liu and C. C. Li, *Green Chem.*, 2023, **25**, 4154–4179.
99 Y. Lu, X. Wu, Z. Li, H. Jiang, L. Liu, Q. Ban and L. Gai, *J. Alloys Compd.*, 2023, **937**, 168344.
100 Q. Gui, Y. Li and J. Liu, *J. Colloid Interface Sci.*, 2024, **662**, 119–128.
101 Z. Guo, Y. Zhao, Y. Ding, X. Dong, L. Chen, J. Cao, C. Wang, Y. Xia, H. Peng and Y. Wang, *Chem*, 2017, **3**, 348–362.
102 J. M. Cao, Y. Liu, K. Li, I. V. Zatovsky, J. L. Yang, H. H. Liu, Z. Y. Gu, X. Gao, K. Y. Zhang, S. H. Zheng and X. L. Wu, *Natl. Sci. Rev.*, 2025, **12**, nwaf074.
103 S. T. Senthilkumar, H. Bae, J. Han and Y. Kim, *Angew. Chem.*, 2018, **130**, 5433–5437.
104 J. Ding, Q. Li, J. Yang, R. Wang, J. Ruan, F. Fang, D. Sun and F. Wang, *Adv. Funct. Mater.*, 2024, **34**, 1–9.
105 W. Liu, Q. Zhao, H. Qi, D. Chen, F. Tang, X. Liu, H. Yu, G. Zhou, Y. Chen and L. Chen, *Chin. Chem. Lett.*, 2025, 110893.
106 X. Li, J. Miao, F. Hu, K. Yan, L. Song, H. Fan, L. Ma and W. Wang, *J. Mater. Chem. A*, 2023, **12**, 968–978.

107 K. Zhu, Z. Sun, Z. Li, P. Liu, X. Chen and L. Jiao, *Energy Storage Mater.*, 2022, **53**, 523–531.
108 S. Wang, N. Hu, Y. Huang and W. Deng, *Appl. Surf. Sci.*, 2023, **619**, 156725.
109 Y. Sun, Y. Zhang, Z. Xu, W. Gou, X. Han, M. Liu and C. M. Li, *ChemSusChem*, 2022, **15**, 6–11.
110 K. K. Abdalla, Y. Wang, K. K. Abdalla, J. Xiong, Q. Li, B. Wang, X. Sun and Y. Zhao, *Sci. China Mater.*, 2024, **67**, 1367–1378.
111 R. Zhang, C. Cui, R. Xiao, R. Li, T. Mu, H. Huo, Y. Ma, G. Yin and P. Zuo, *Chem. Eng. J.*, 2022, **451**, 138663.
112 N. S. Alghamdi, D. Rakov, X. Peng, J. Lee, Y. Huang, X. Yang, S. Zhang, I. R. Gentle, L. Wang and B. Luo, *Angew. Chem.*, 2025, **64**, e202502739.
113 Z. Bin Wang, J. Zhang, Q. Miao, H. Y. Cao, F. Xiong, T. Lee, A. El-Baz, L. Xie and S. Q. Ni, *Environ. Sci. Technol.*, 2024, **58**, 21242–21250.
114 Y. Quan, M. Yang, M. Chen, W. Zhou, X. Han, J. Chen, B. Liu, S. Shi and P. Zhang, *Chem. Eng. J.*, 2023, **458**, 141392.
115 Y. Cheng, X. Chi, J. Yang and Y. Liu, *J. Energy Storage*, 2021, **40**, 102701.
116 Q. Gao, Z. Chen, J. Feng, X. Zhou, Z. Wan, L. Zhang, H. Gu, L. Sheng, P. Yao, F. R. Wang and Z. Hao, *Green Chem.*, 2025, **27**, 3990–3999.
117 J. Feng, Z. Chen, W. Zhou and Z. Hao, *Mater. Horiz.*, 2023, **10**, 4686–4709.
118 H. J. Liang, H. H. Liu, J. Z. Guo, X. X. Zhao, Z. Y. Gu, J. L. Yang, X. Y. Zhang, Z. M. Liu, W. L. Li and X. L. Wu, *Energy Storage Mater.*, 2024, **66**, 103230.
119 J. Liu, X. Li, D. Wu, H. Wang, J. Huang and J. Ma, *Acta Phys.-Chim. Sin.*, 2024, **40**, 1–9.
120 D. Hubble, D. E. Brown, Y. Zhao, C. Fang, J. Lau, B. D. McCloskey and G. Liu, *Energy Environ. Sci.*, 2022, **15**, 550–578.
121 C. Chen, Y. Li, C. Wang, H. He, M. Liu and Y. B. He, *Battery Energy*, 2024, 1–12.
122 F. Huang, Y. J. Guo, W. Zhao, R. Wu, Y. Dong, G. Long and P. Du, *Chem. Eng. J.*, 2024, **498**, 155248.
123 D. W. Park, M. W. Chung, S. K. Kim and Y. K. Choi, *J. Korean Chem. Soc.*, 2008, **52**, 676–683.
124 Z. Ye, M. Yang, Y. Guo, Y. Chen, B. Zhang, S. Liu, Y. Chen and W. Guo, *ACS Appl. Polym. Mater.*, 2024, **6**, 11901–11910.
125 Y. Chen, H. Ren, D. Rong, Y. Huang, S. He and Q. Rong, *Polymer*, 2023, **270**, 125796.
126 J. Wang, C. Gao, P. Hou, Y. Liu, J. Zhao and P. Huo, *Chem. Eng. J.*, 2023, **455**, 140952.
127 W. Viola and T. L. Andrew, *J. Phys. Chem. C*, 2021, **125**, 246–251.
128 S. Dai, X. Hu, X. Xu, X. Cao, Y. Chen, X. Zhou, J. Ding and N. Yuan, *Synth. Met.*, 2019, **257**, 116177.
129 Q. Chen, L. Wang and J. Chen, *ChemElectroChem*, 2022, **9**, 1–5.
130 Z. Liu, J. Zhang, J. Liu, Y. Long, L. Fang, Q. Wang and T. Liu, *J. Mater. Chem. A*, 2020, **8**, 6219–6228.
131 Z. Chen, J. Feng, W. Zhou, J. Lu, J. Cai, L. Zhang, L. Sheng, H. Gu, P. Yao, F. R. Wang and Z. Hao, *ACS Appl. Mater. Interfaces*, 2024, **16**, 53801–53810.
132 Z. Chen, J. Feng, P. Yao, J. Cai, W. Zhou, J. Lu, L. Zhang, L. Sheng, H. Gu, F. R. Wang and Z. Hao, *Electrochim. Acta*, 2024, **508**, 145291.
133 Y. He, Z. Chen, J. Feng, J. Wang, L. Zhang, H. Gu, L. Sheng, P. Yao, F. R. Wang and Z. Hao, *Small*, 2025, **2411755**, 1–11.
134 W. Cheng, M. Zhao, Y. Lai, X. Wang, H. Liu, P. Xiao, G. Mo, B. Liu and Y. Liu, *Exploration*, 2023, **4**, 20230056.
135 X. Wang, Y. Zhang, L. Guo, J. Li, P. Wang, L. Yang and Z. Liu, *Chin. Chem. Lett.*, 2025, **36**, 111231.